Supplementary Material (ESI) for Chemical Communications

Supporting Information for

Remarkably Bistable and Fast Reversible Calixarene Based Copper Centered Redox Molecular Switch

Ulrich Darbost,* Vanessa Penin, Erwann Jeanneau, Caroline Félix, Francis Vocanson, Christophe Bucher, Guy Royal and Isabelle Bonnamour

E-mail : ulrich.darbost@univ-lyon1.fr

Outline:

General methods. Solvents were purified and dried by standard methods prior to use. All reactions were carried out under nitrogen. Column chromatography was performed using silica gel (Kieselgel-60, 0.040-0.063 nm, Merck). Reactions were monitored by TLC on POLYGAM® SIL G/UV_{254} (Macherey-Nagel) silica gel plate and visualized by UV light. ^{1}H NMR and ^{13}C NMR spectra were recorded at 300 and 75 MHz ($CDCl_3$) on a Bruker Avance DRX 300 spectrometer. Mass spectra were acquired on a ThermoFinnigan LCQ Advantage ion trap instrument, detecting positive ions (+) or negative ions (-) in the ESI mode. Samples (in methanol:dichloromethane:water, 45:40:15, v/v/v) were infused directly into the source (5µL/min) using a syringe pump. The following source parameters were applied: spray voltage 3.0–3.5 kV, nitrogen sheath gas flow 5–20 arbitrary units. The heated capillary was held at 200°C. High resolution mass spectra were acquired on a THERMOQUEST Finnigan MAT 95 XL. Acetonitrile (Rathburn, HPLC grade) was used as received. Tetra-*n*-butylammonium PF_6 was purchased from Fluka and used as recieved. Electrochemical experiments were conducted in a conventional three-electrode cell. For analytical experiments, the counter electrode was a platinum wire. The reference electrode was a $Ag/AgNO_3$ (10 mM in CH_3CN containing 0.1 M TBAP) purchased from CH-instrument. Rotating disk electrode (RDE) voltammetry was carried out with a radiometer equipment at a rotation rate of 500 rpm using glassy carbon RDE tips (Ø = 2 mm). Cyclic voltammetry (CV) curves were recorded using a CH instrument CH-660 potentiostat. The CH-intrument vitreous carbon working electrodes ((Ø = 2 mm). were polished with 1 μm diamond paste before each recording. Electrolyses were performed at controlled

potential using a Pt plate as working electrode as well as a large Pt counter electrode isolated through an ionic bridge.

Synthesis of Di-quinoline calixarene 2

Under nitrogen atmosphere, dibromo calixarene **1** (4.25 g ; 4.62 mmol ; 1 equiv) and K_2CO_3 (2.55 g ; 18.5 mmol ; 4 equiv) were dissolved in freshly distillate acetonitrile (80 mL). The suspension was stirring during 30 minutes at room temperature. 8-hydroxyquinoline (5,36 g ; 37,0 mmol ; 8 éq.) was then added and the reaction mixture was refluxing during 5 days. After allowing the mixture going back to room temperature, the solvent was removed under reduced pressure and the resulting residue was dissolved in dichloromethane and wash with HCl 10 % (100 mL), then with water until pH = 7. After dichloromethane extraction, drying, filtration and solvent evaporation, the resulting crude compound was purified by flash chromatography (methanol/dichloromethane 3/97) giving pure diquinoleine calixarene **2** (3.09 g, 64 %) as pale beige solid: mp 190 °C dec; IR ($CHCl_3$) ν 3403, 2952, 1485, 1318, 1111, 745 cm^{-1}; ^1H NMR ($CDCl_3$) δ 0.89 (s, 18 H, tBu), 1.22 (s, 18H, tBu), 2.17-2.22 (m, 4H, O-CH_2-CH_2-*CH_2*-CH_2-O-quino), 2.28-2.34 (m, 4H, O-CH_2-C*H_2*-*C*H_2-CH_2-O-quino), 3.24 (d, 4H, *J* = 13 Hz, Ar-*CH_2*-Ar ax), 4.00 (t, 4H, *J* = 6.2 Hz, O-CH_2-CH_2-*C*H_2-C*H_2*-O-quino), 4.20 (d, 4H, *J* = 13 Hz, Ar-*CH_2*-Ar eq), 4.31 (t, 4H, *J* = 5.9 Hz, O-C*H_2*-CH_2-*C*H_2-CH_2-O-quino), 6.73 (s, 4H, Ar*H_{calix}*), 6.98 (s, 4H, Ar*H_{calix}*), 7.06 (sl, 2H, *$H_{quinoline}$*), 7.29-7.38 (m, 6H, *$H_{quinoline}$*), 7.49 (s, 2H, O*H*) ; 8.10 (d, 2H, *J* = 7 Hz, *$H_{quinoline}$*), 8.91 (m, 2H, *$H_{quinoline}$*); ^{13}C NMR ($CDCl_3$) δ 26.2, 27.3, 31.4, 32.1, 34.2, 34.3, 68.9, 76.5, 109.4, 119.8, 121.8, 125.5, 125.9, 127.2, 128.2, 129.9, 133.0, 136.2, 140.8, 141.8, 147.2, 149.6, 150.3, 151.1, 155.2. HRMS (ESI-TOF) m/z : calcd for $C_{70}H_{83}N_2O_6$ $[M + H]^+$: 1047.6251; Found: 1047.6244.

Synthesis of [di-quino di-imidazole] calixarene 3

Under nitrogen atmosphere, anhydrous THF was added to a mixture of di-quinoline calixarene **2** (2.00 g; 1.91 mmol) and NaH (60% in oil, 1.38 g, 34.5 mmol). The reaction mixture was stirred for one hour at room temperature and 2-chloromethyl-*N*-methylimidazole hydrochloride (1.92 g, 11.5 mmol) was introduced. After 18 h of refluxing, the solvent was removed under reduced pressure and the resulting residue was dissolved in dichloromethane and washed with water until pH = 7. After dichloromethane extraction drying, filtration and solvent evaporation, the resulting crude compound was purified by flash chromatography (dichlorométhane/méthanol/triéthylamine : 88/10/2) giving pure di-imidazole di-quinoline calixarene **3** (1.13 g, 48 %) as a white solid: mp 194 °C ; IR ($CHCl_3$) ν 2959, 1479, 1260, 1105, 791 cm^{-1}; ^1H NMR ($CDCl_3$) δ 0.79 (s, 18 H, tBu), 1.22 (s, 18H, tBu), 1.79-1.90 (m, 4H, O-CH_2-

CH_2-*CH_2*-CH_2-O-quino), 1.95-2.05 (m, 4H, O-CH_2-C*H_2*-*C*H_2*-CH_2-O-quino), 2.99 (d, 4H, *J* = 13 Hz, Ar-*CH_2*-Ar ax), 3.46 (s, 6H, NC*H_3*), 3.90 (t, 4H, *J* = 5.9 Hz, O-C*H_2*-CH_2-CH_2-CH_2-O-quino), 4.09 (t, 4H, *J* = 6.2 Hz, O-CH_2-CH_2-*C*H_2*-C*H_2*-O-quino), 4.30 (d, 4H, *J* = 13 Hz, Ar-*CH_2*-Ar eq), 4.78 (s, 4H, C*H_2*Im), 6.44 (s, 4H, Ar*H_{calix}*), 6.70 (s, 2H, Im*H*), 6.88 (s, 2H, Im*H*), 6.97 (s, 4H, Ar*H_{calix}*), 7.02 (d, 2H, *J* = 7.0 Hz, *$H_{quinoline}$*), 7.20-7.34 (m, 6H, *$H_{quinoline}$*), 8.03 (d, 2H, *J* = 7 Hz, *$H_{quinoline}$*), 8.83-8.84 (m, 2H, *$H_{quinoline}$*); ^{13}C NMR ($CDCl_3$) δ 26.2, 26.8, 31.3, 31.6, 32.1, 33.2, 34.1, 34.4, 67.7, 69.5, 75.0, 109.4, 119.7, 121.9, 125.1, 125.8, 125.8, 128.5, 129.9, 132.9, 135.5, 136.2, 140.8, 145.1, 145.3, 149.5, 151.8, 154.7, 155.3. HRMS (ESI-TOF) m/z : calcd for $C_{80}H_{95}N_6O_6$ $[M + H]^+$: 1235.7313; Found: 1235.7313.

Synthesis of complex 3.Cu I

Under nitrogen, $CHCl_3$ (3 mL) was added to a mixture of di-quino di-midazole calixarene **3** (30.0 mg, 0.024 mmol) and $[Cu(CH_3CN)_4]PF_6$ (9.5 mg, 0.025 mmol). The resulting pale yellow solution was stirring for one hour at room temperature. After a removal of the solvent under reduces pressure, the obtained complex **3.Cu I** was dry under vacuum. (31 mg, 88 %): mp 155 °C dec; IR ($CHCl_3$) ν 2953, 1571, 1502, 1479, 837 cm^{-1}; ^{1}H NMR ($CDCl_3$) δ 0.81 (s, 18 H, tBu), 1.37 (s, 18H, tBu), 1.90-2.20 (m, 8H, O-CH_2-C*H_2*-*CH_2*-CH_2-O-quino), 3.02 (s, 6H, NC*H_3*), 3.11 (d, 4H, *J* = 13 Hz, Ar-*CH_2*-Ar ax), 3.70-3.80 (m, 4H, O-C*H_2*-CH_2-CH_2-CH_2-O-quino), 3.95 (d, 4H, *J* = 13 Hz, Ar-*CH_2*-Ar eq), 4.30-4.40 (m, 4H, O-CH_2-CH_2-*C*H_2*-C*H_2*-O-quino), 5.45-5.55 (m, 4H, C*H_2*Im), 6.36 (s, 4H, Ar*H_{calix}*), 6.80-7.00 (m, 4H, Im*H*), 7.14 (s, 4H, Ar*H_{calix}*), 7.18 (d, 2H, *J* = 8.4 Hz, *$H_{quinoline}$*), 7.30-7.55 (m, 6H, *$H_{quinoline}$*), 8.12 (d, 2H, *J* = 8.1 Hz, *$H_{quinoline}$*), 8.80 (d, 2H, *J* = 4.6 Hz, *$H_{quinoline}$*); ^{13}C NMR ($CDCl_3$) δ 26.5, 27.8, 31.5, 31.7, 32.1, 34.0, 34.6, 71.0, 109.7, 120.1, 122.2, 124.9, 126.7, 127.6, 130.0, 131.6, 135.9, 136.6, 140.1, 145.0, 147.2, 149.7, 150.4, 153.8, 154.8. HRMS (ESI-TOF) m/z: calcd for $C_{80}H_{94}CuN_6O_6$ $[M]^+$: 1297.6531; Found: 1297.6528.

Synthesis of complex 3.Cu II

Under nitrogen, CH_3CN (3 mL) was added to a mixture of di-quino di-midazole calixarene **3** (32.1 mg, 0.026 mmol) and $Cu(ClO_4)_2$,$6H_2O$ (9.8 mg, 0.026 mmol). The resulting deep green solution was stirring for one hour at room temperature. After a removal of the solvent under reduces pressure, the obtained complex **3.Cu II** was dry under vacuum. (32 mg, 82 %): mp 190 °C dec; IR ($CHCl_3$) ν 2954, 1585, 1509, 1479, 1083 cm^{-1}; HRMS (ESI-TOF) m/z: calcd for $C_{80}H_{94}ClCuN_6O_{10}$ $[M\text{-}ClO_4]^+$: 1396.6016; Found: 1396.6018; UV-vis (λ_{max} = 635 nm, ε = 62.4 $M^{-1}.cm^{-1}$). EPR: (9.44 GHz, 40K, CH_3CN/Toluene 1/1, v/v): $A_{//}$ = 172 10^{-4} cm^{-1} $g_{//}$ = 2.211 $g_{\perp}$ = 2.004.

Crystallographic data

A suitable crystal was mounted on a Nonius KappaCCD diffractometer using Mo Kα radiation (λ = 0.71073 Å). Intensities were collected at 150(1) K for CCDC 727116 and 293(2) K for CCDC 727115 by means of the COLLECT software.[1] Reflection indexing, Lorentz-polarization correction, peak integration, and background determination were carried out with DENZO.[2] Frame scaling and unit-cell parameters refinement were made with SCALEPACK.[2] A semi-empirical absorption correction was applied using the program DIFABS [3]. The structures were solved by direct methods with SIR97.[4] The remaining non-hydrogen atoms were located by successive difference Fourier map analyses. H-atoms were placed geometrically and included in the refinement using soft restraints on the bond lengths and angles to regularize their geometry (C-H in the range 0.93-0.98 Å and O-H = 0.82 Å) and isotropic atomic displacement parameters (U(H) in the range 1.2-1.5 times $U_{eq.}$ of the adjacent atom). In the last cycles of the refinement, the hydrogen atoms were refined using a riding mode. The structure refinement was carried out with CRYSTALS.[5]

[1] Nonius, B. V. *COLLECT*; Nonius: Delft, The Netherlands, 1997-2001.
[2] Otwinowski, Z.; Minor, W. *Methods in Enzymology*; Carter, C. W., Jr., Sweet, R. M., Eds.; Academic Press: New York, 1997; Vol. *276*, pp 307-326.
[3] Walker N. and Stuart D., *Acta Crystallogr*., Sect A **1983**, 39, 158-166.
[4] Altomare, A.; Burla, M. C.; Camalli, M.; Cascarano, G. L.; Giacovazzo, C.; Guagliardi, A.; Moliterni, A. G. G.; Polidori, G.; Spagna, R. *J. Appl. Crystallogr.* **1999**, *32*, 115–119.
[5] Betteridge, P. W.; Carruthers, J. R.; Cooper, R. I.; Prout, K. and Watkin, D. J. *J. Appl. Crystallogr.* **2003**, *36*, 1487.

Table S1. Selected Crystal data for [**3.**Cu(II)H_2O]$(ClO_4)_2$

Empirical formula	$C_{80}H_{96}CuN_6O_7.C_4H_{10}O.5(C_2H_3N).2(ClO_4)$	
Formula weight	1795.51 g/mol	
Temperature	150(2) K	
Wavelength	0.71073 Å	
Crystal system	Triclinic	
Space group	*P* -1	
Unit cell dimensions	a = 11.4073(2) Å	α = 90.6330(10) °.
	b = 15.2526(3) Å	β = 93.9510(10) °.
	c = 29.7017(8) Å	γ = 112.043(2) °.
Volume	4774.88(19) $Å^3$	
Z	2	
Density (calculated)	1.249 Mg/m^3	
Absorption coefficient	0.35 mm^{-1}	
F(000)	1906	
Crystal size	0.07000 x 0.1100 x 0.1200 mm^3	
Theta range for data collection	0.7 to 28.6 °.	
Index ranges	$0 \le h \le 15, -20 \le k \le 18, -40 \le l \le 39$	
reflections	12327 with $I > 2.0\sigma(I)$,	

Table S2. Selected Crystal data for [**3.**Cu(I)]PF_6

Empirical formula	$C_{80}H_{93}CuN_6O_6 \cdot F_6P$	
Formula weight	1443.13 g/mol	
Temperature	293 K	
Wavelength	0.71069 Å	
Crystal system	Monoclinic	
Space group	*P* 2_1	
Unit cell dimensions	a = 14.399(5) Å	α = 90 °.
	b = 32.127(6) Å	β = 110.3(1) °.
	c = 19.851(9) Å	γ = 90 °.
Volume	8614(5) $Å^3$	
Z	4	
Density (calculated)	1.113 Mg/m^3	
Absorption coefficient	0.330 mm^{-1}	
F(000)	3044	
Crystal size	0.04 x 0.05 x 0.12 mm^3	
Theta range for data collection	1.1 to 22.5 °.	
Index ranges	-15 ≤ h ≤ 14, 0 ≤ k ≤ 34, 0 ≤ l ≤ 21	
reflections	6483 with $I > 2.0\sigma(I)$,	

Figure S1: ^{1}H NMR Spectrum of compound **2**

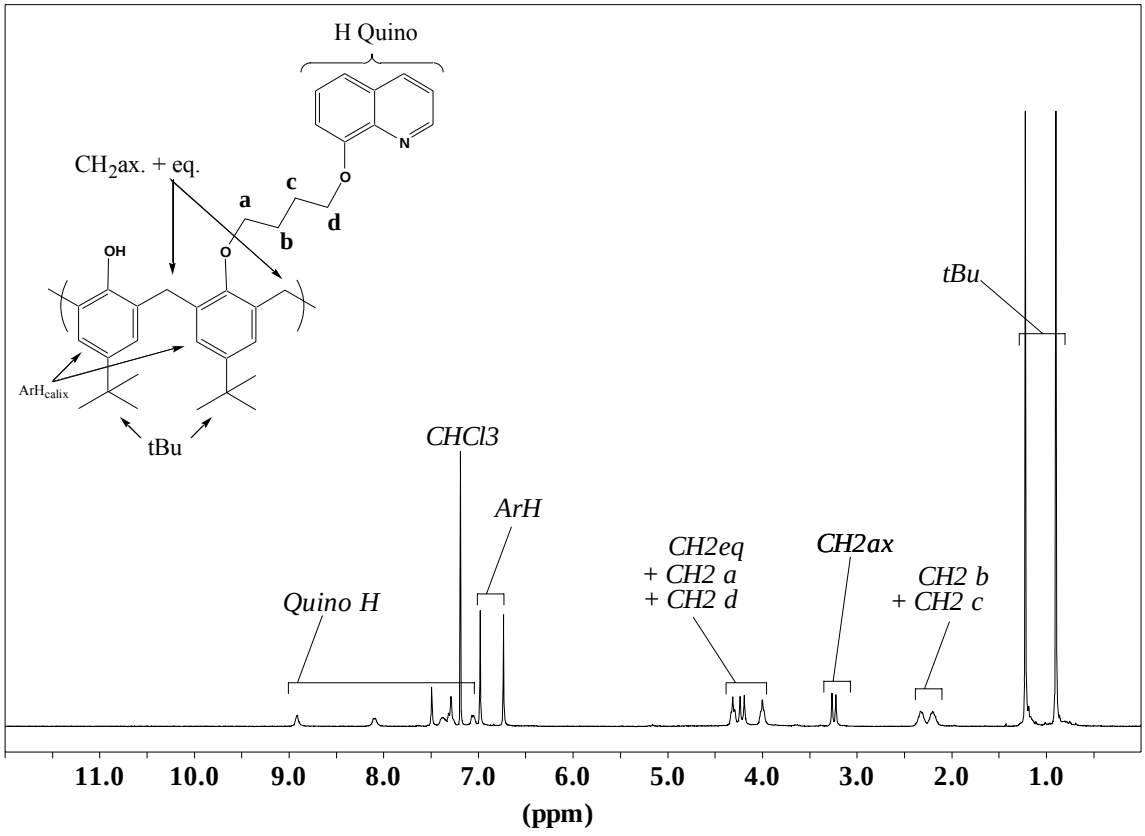

Figure S2: ^{13}C NMR Spectrum of compound **2**

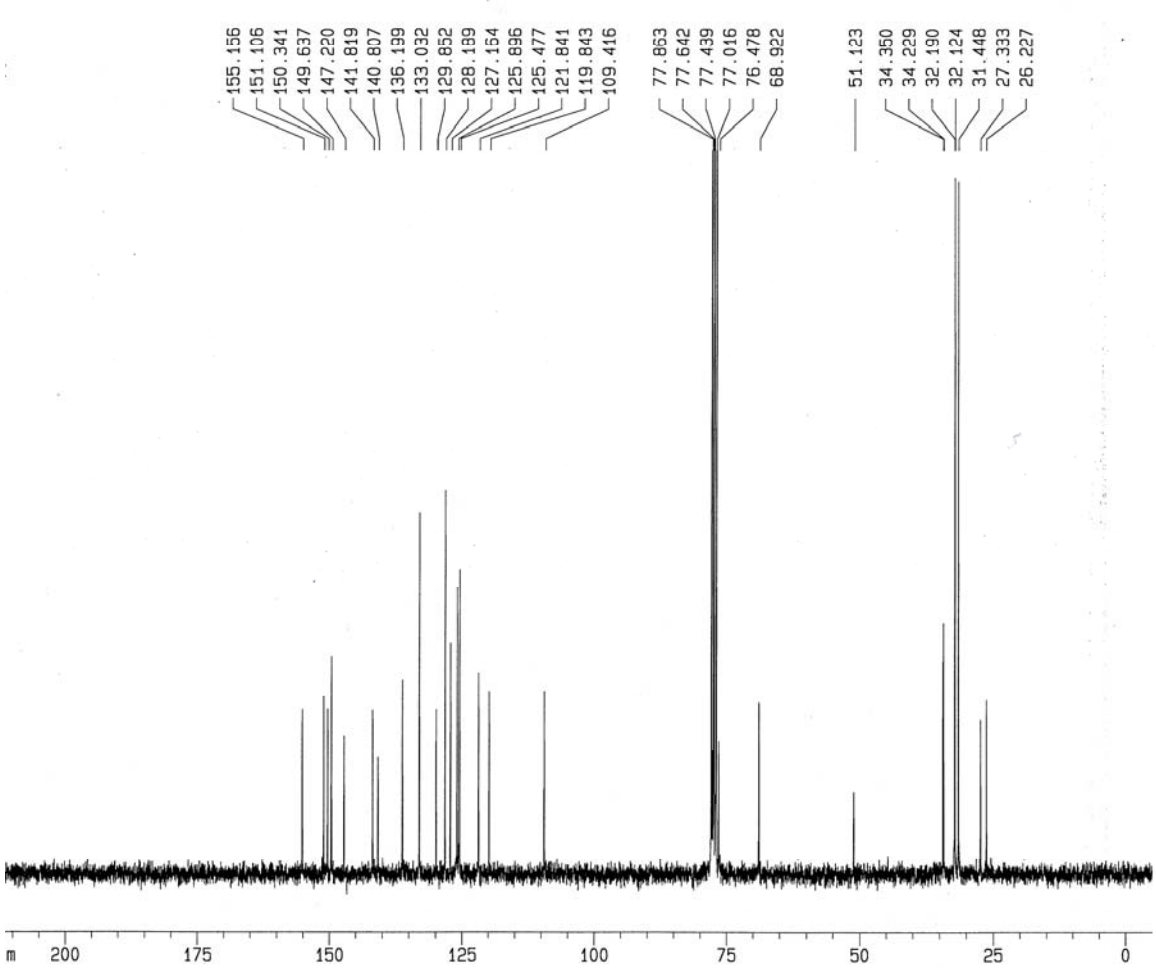

Figure S3: ^{13}C-DEPT NMR Spectrum of compound **2**

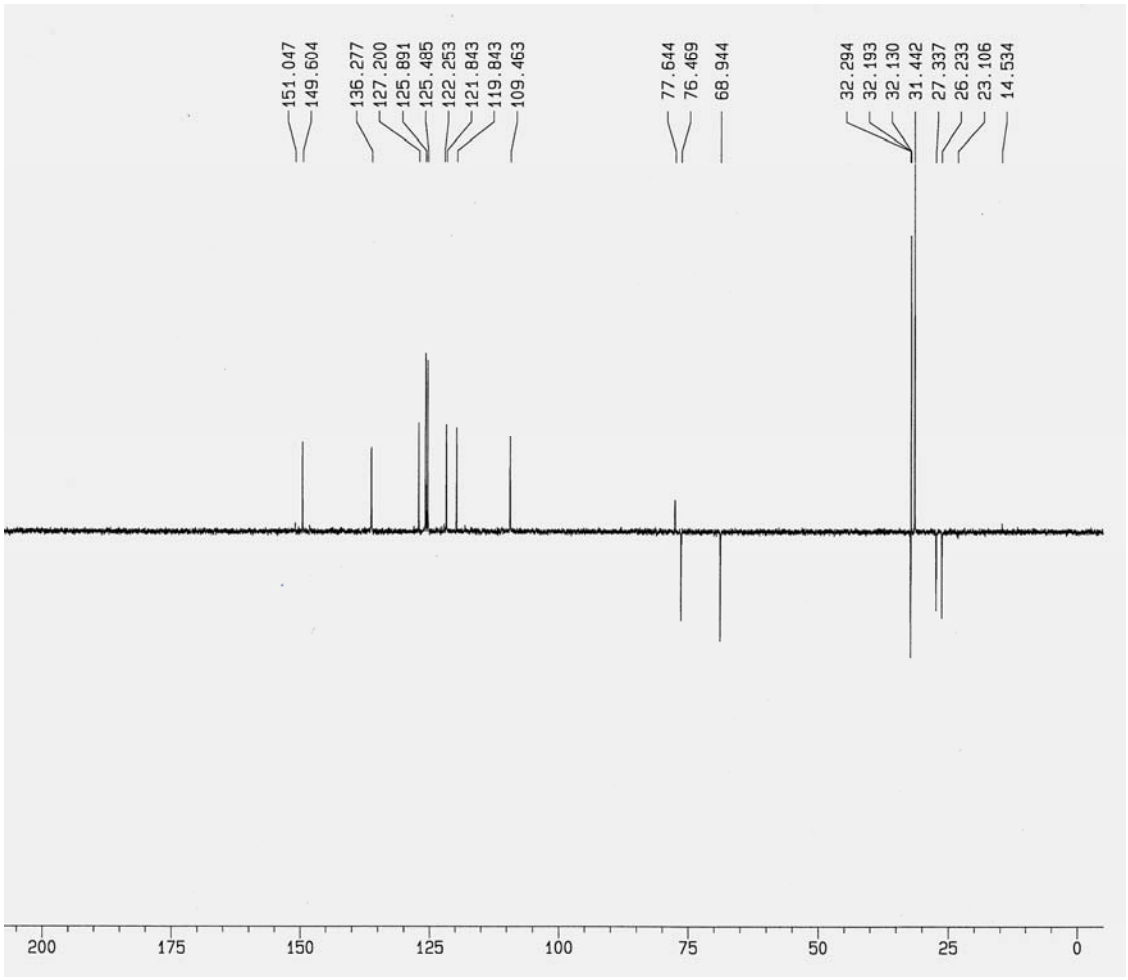

Figure S4: COSY-2D NMR Spectrum of compound **2**

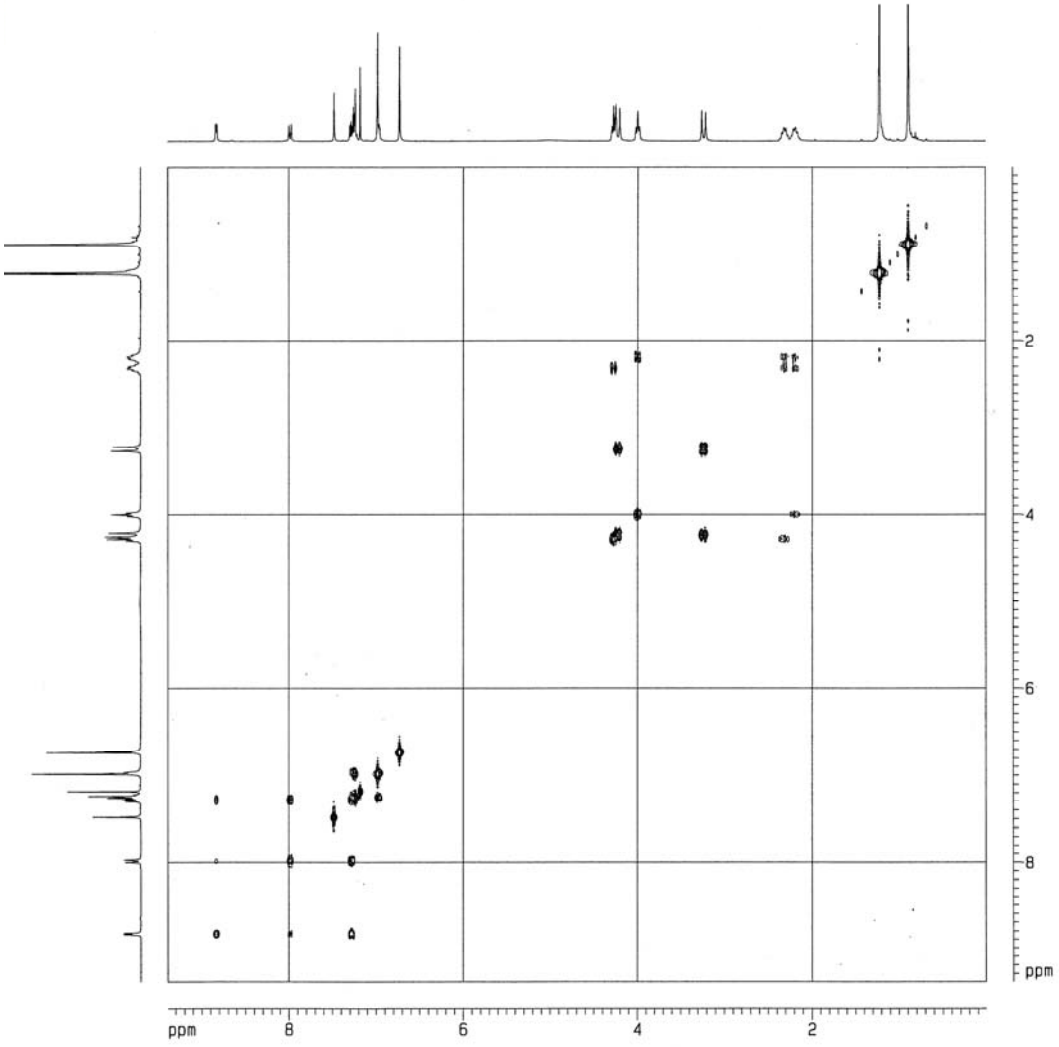

Figure S5: HSQC Spectrum of compound **2**

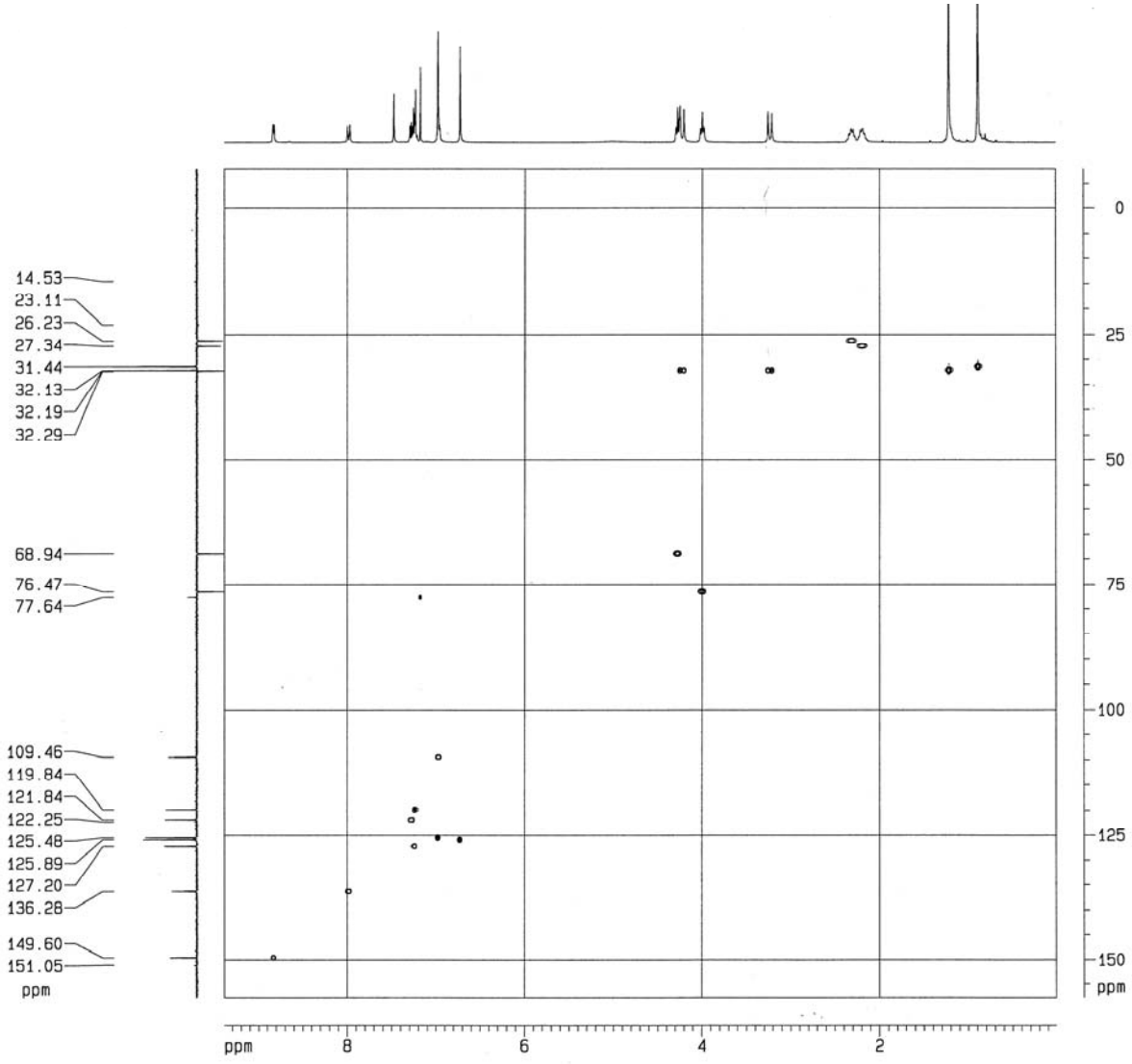

Figure S6: Mass Spectrum of compound **2**

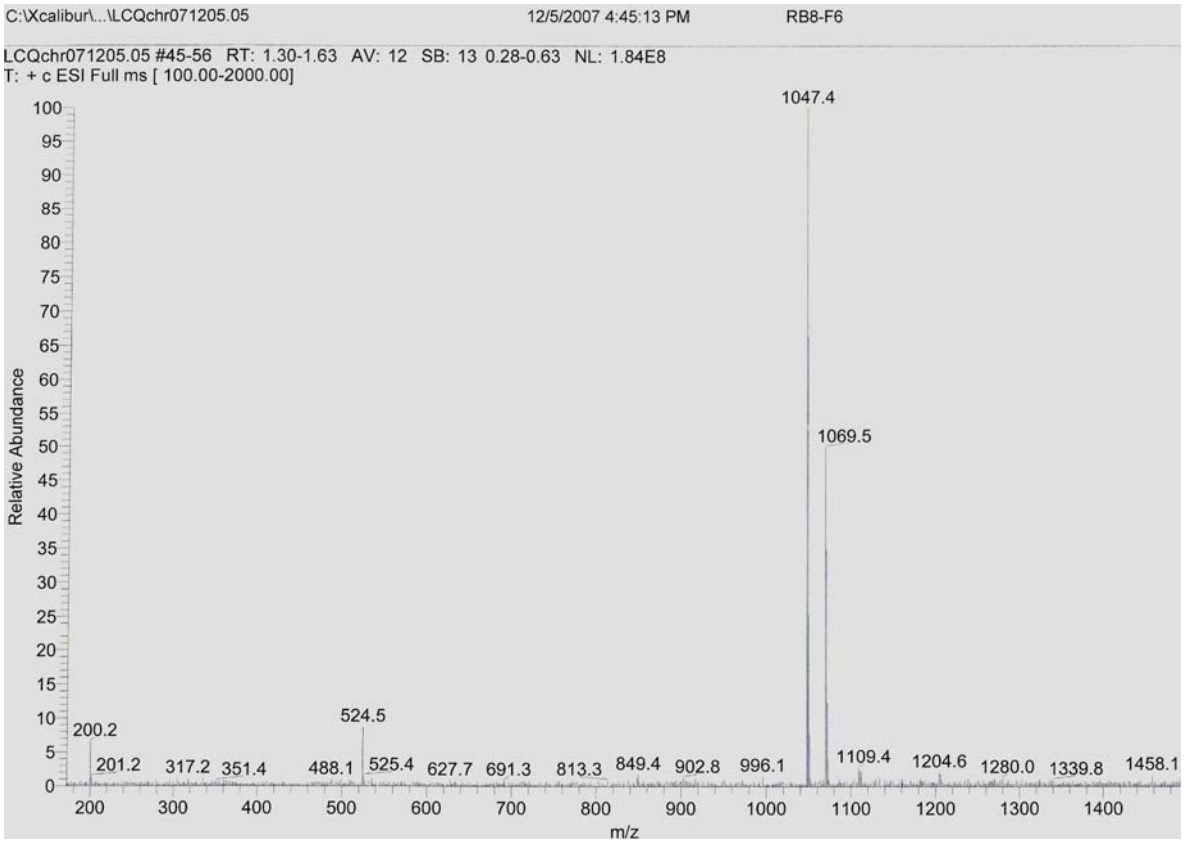

Figure S7: IR Spectrum of compound **2**

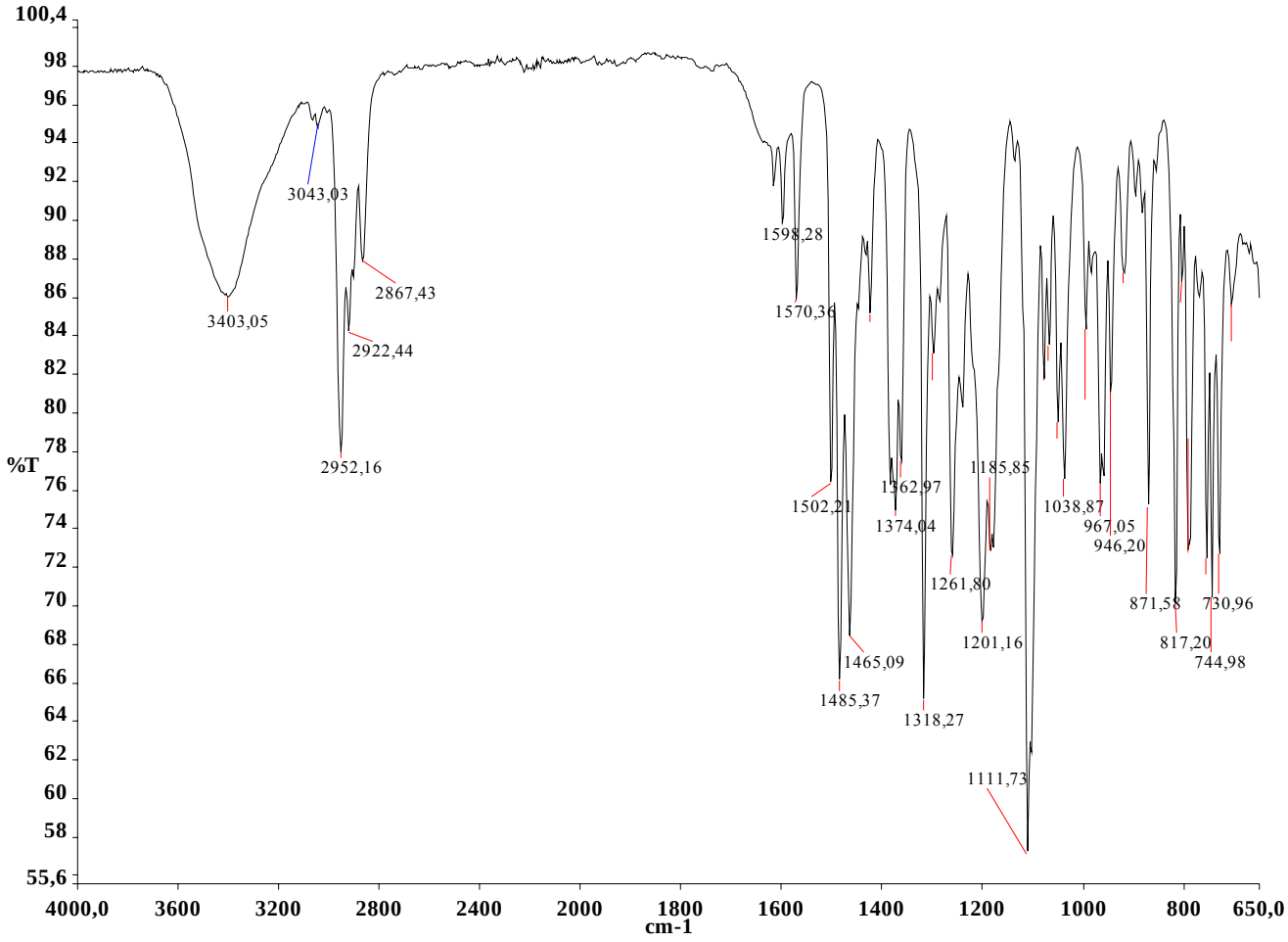

Figure S8: ^{1}H NMR Spectrum of compound **3**

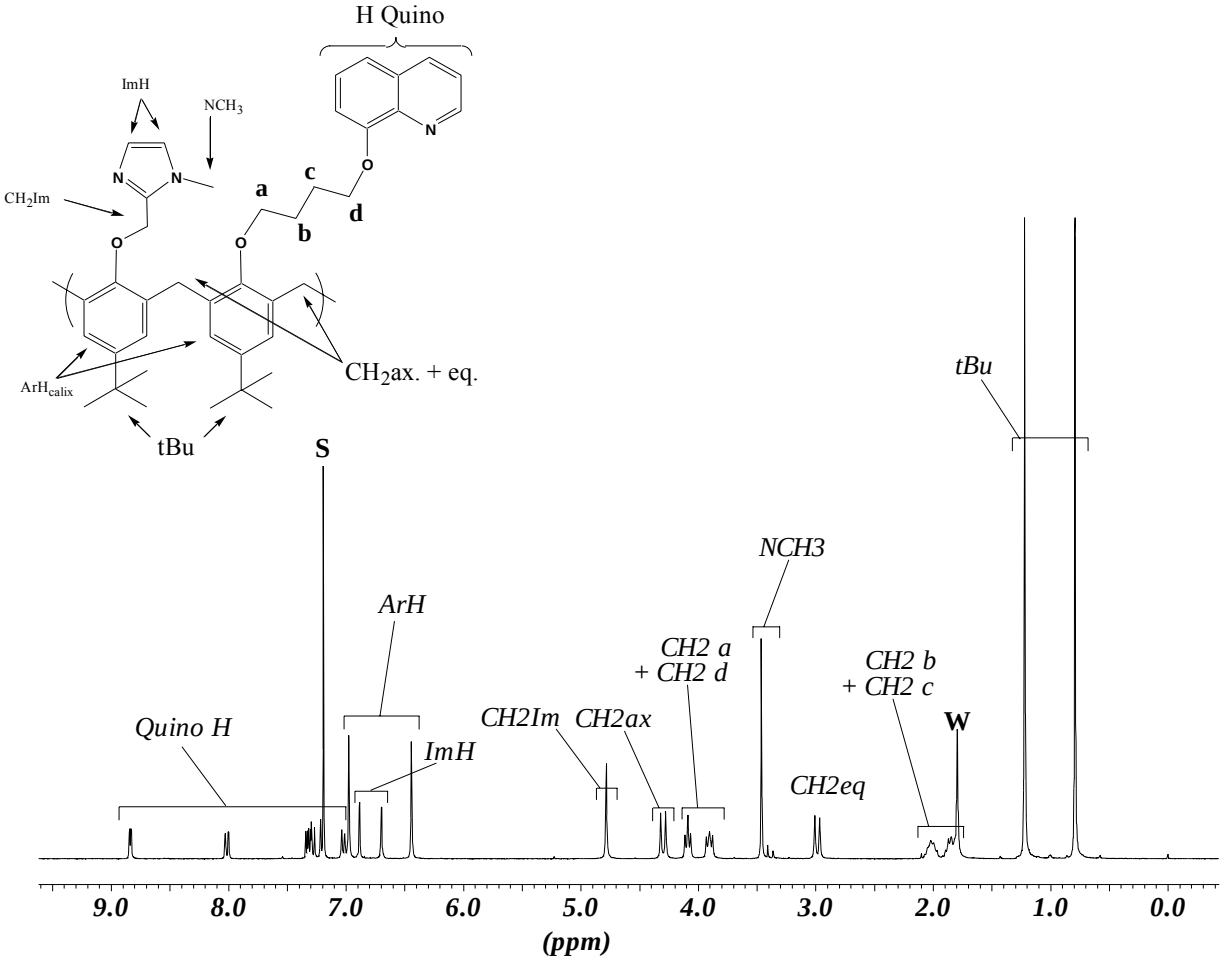

Figure S9: ^{13}C NMR Spectrum of compound **3**

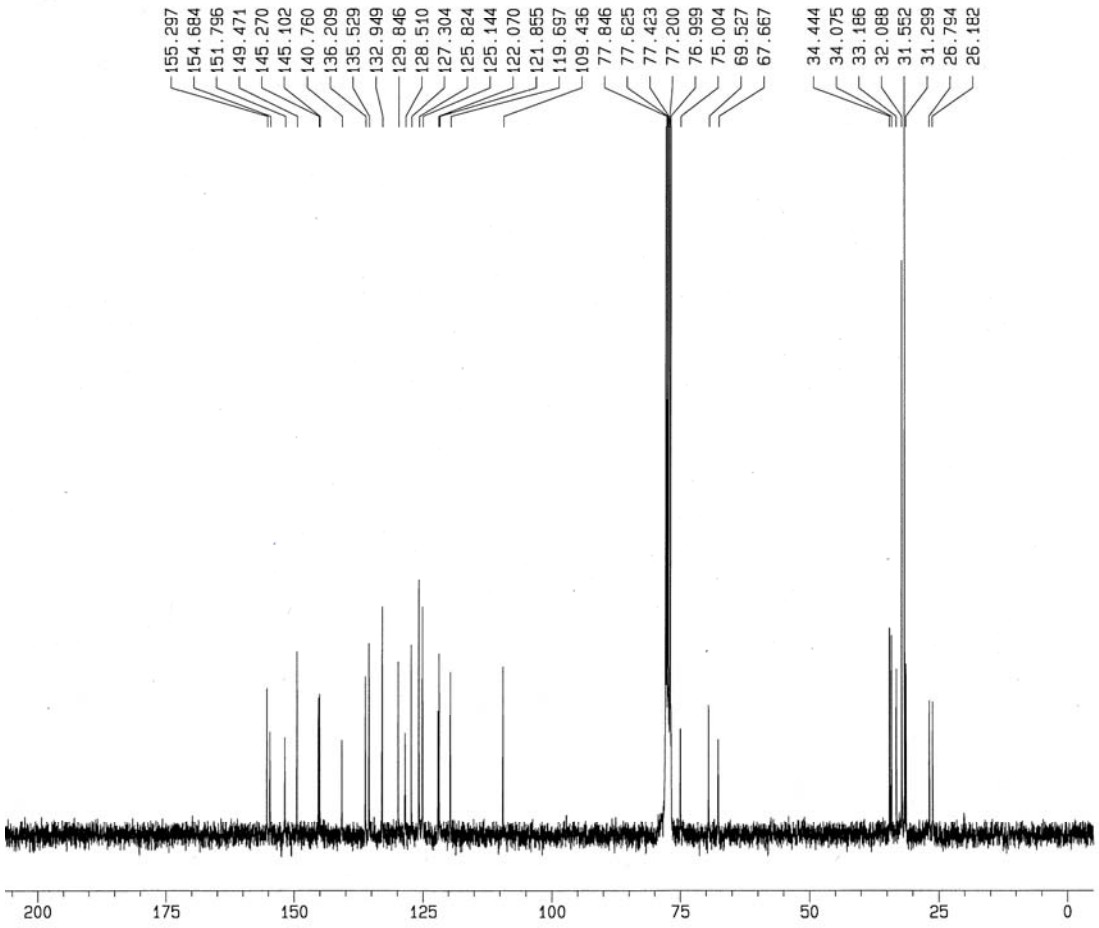

Figure S10: ^{13}C-DEPT NMR Spectrum of compound **3**

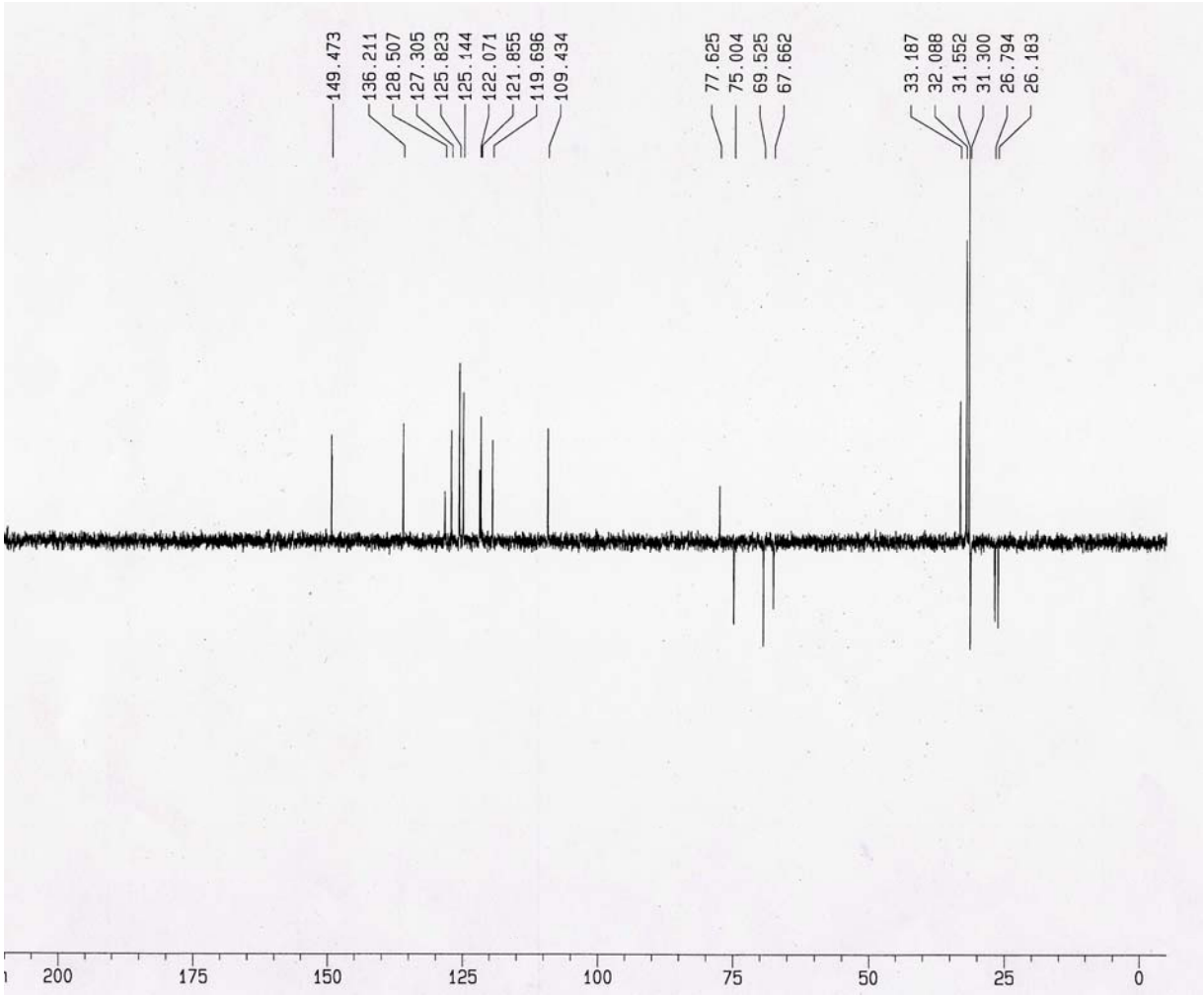

Figure S11: COSY NMR Spectrum of compound **3**

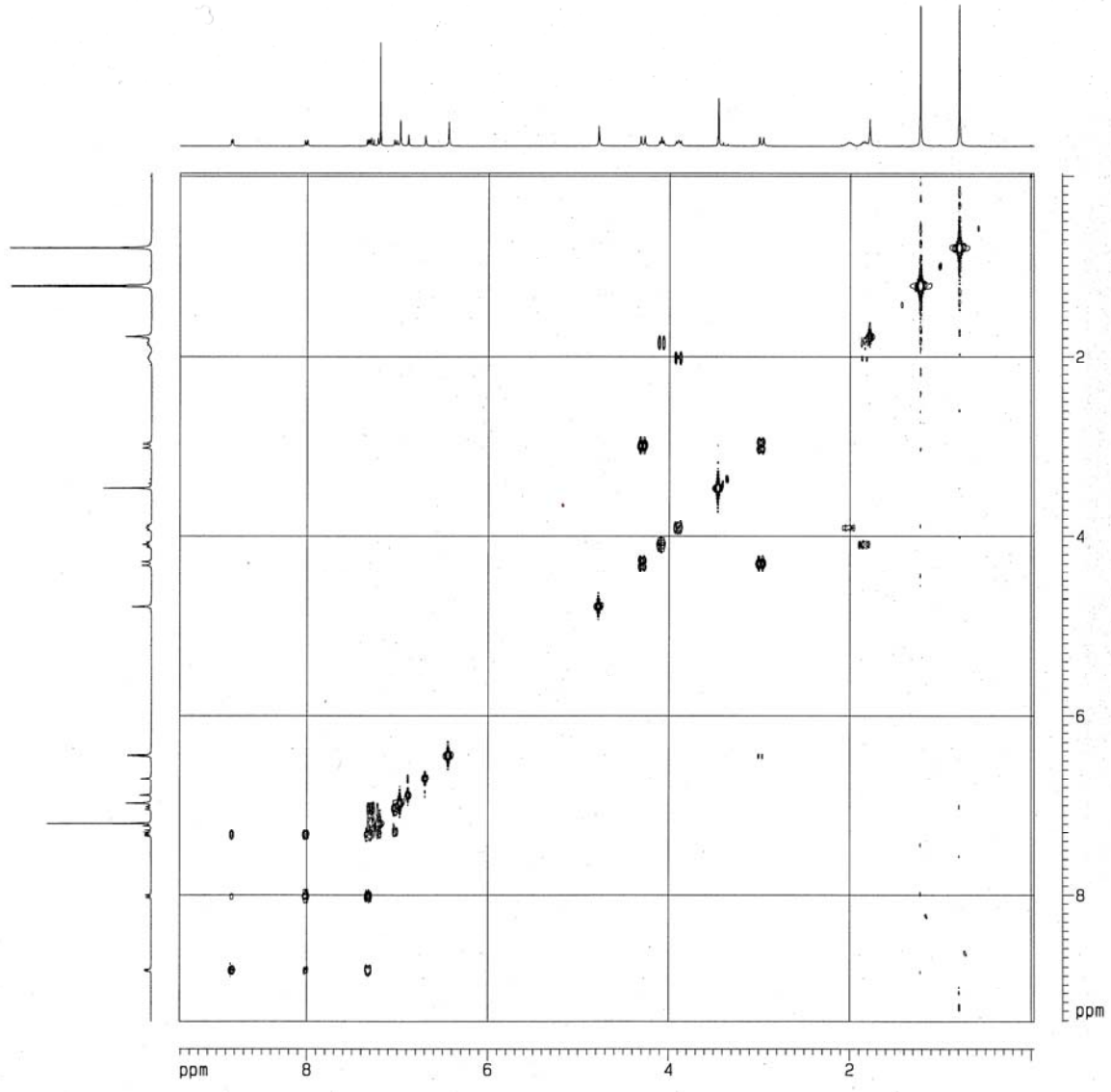

Figure S12: HSQC NMR Spectrum of compound **3**

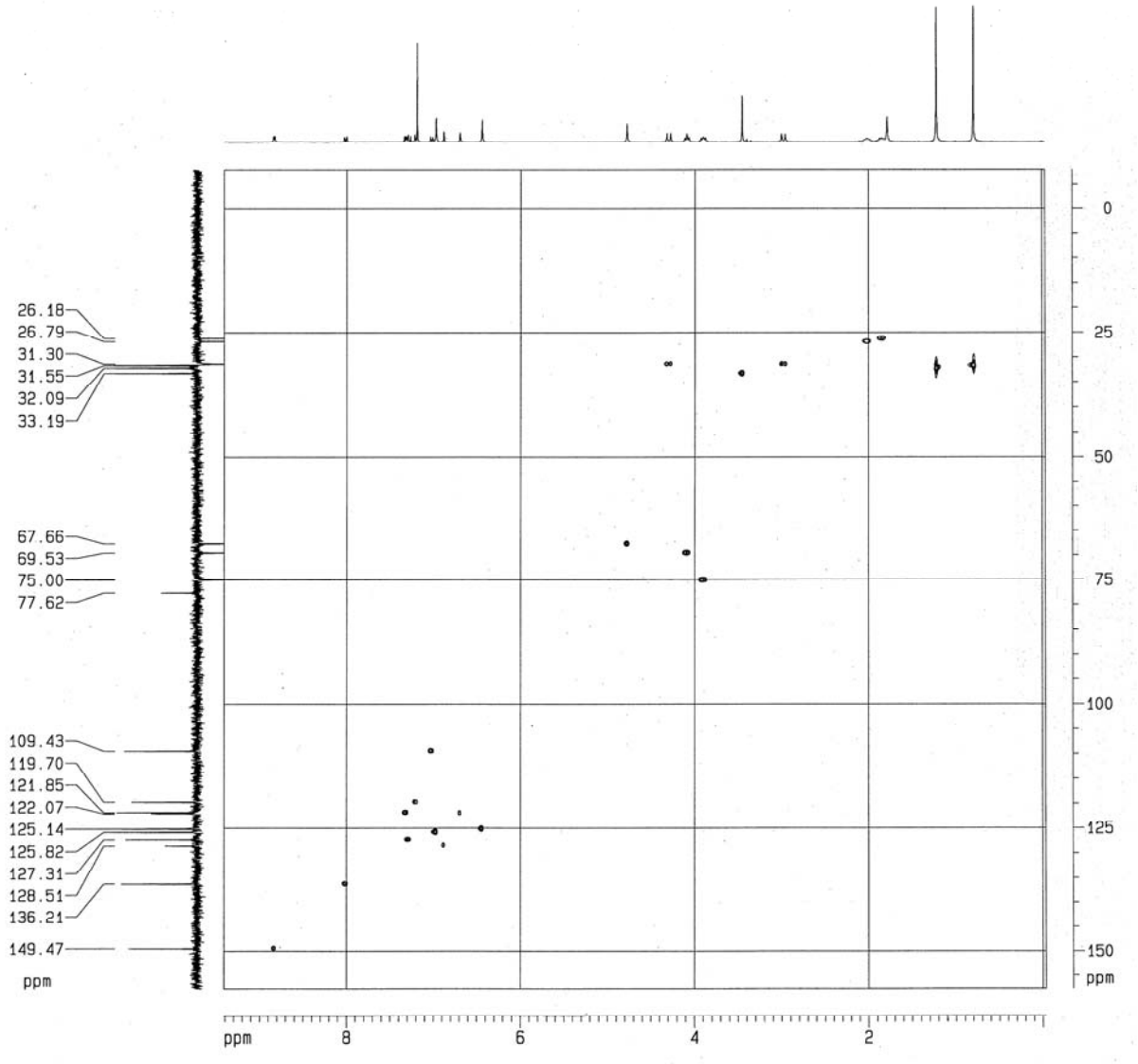

Figure S13: Mass Spectrum of compound **3**

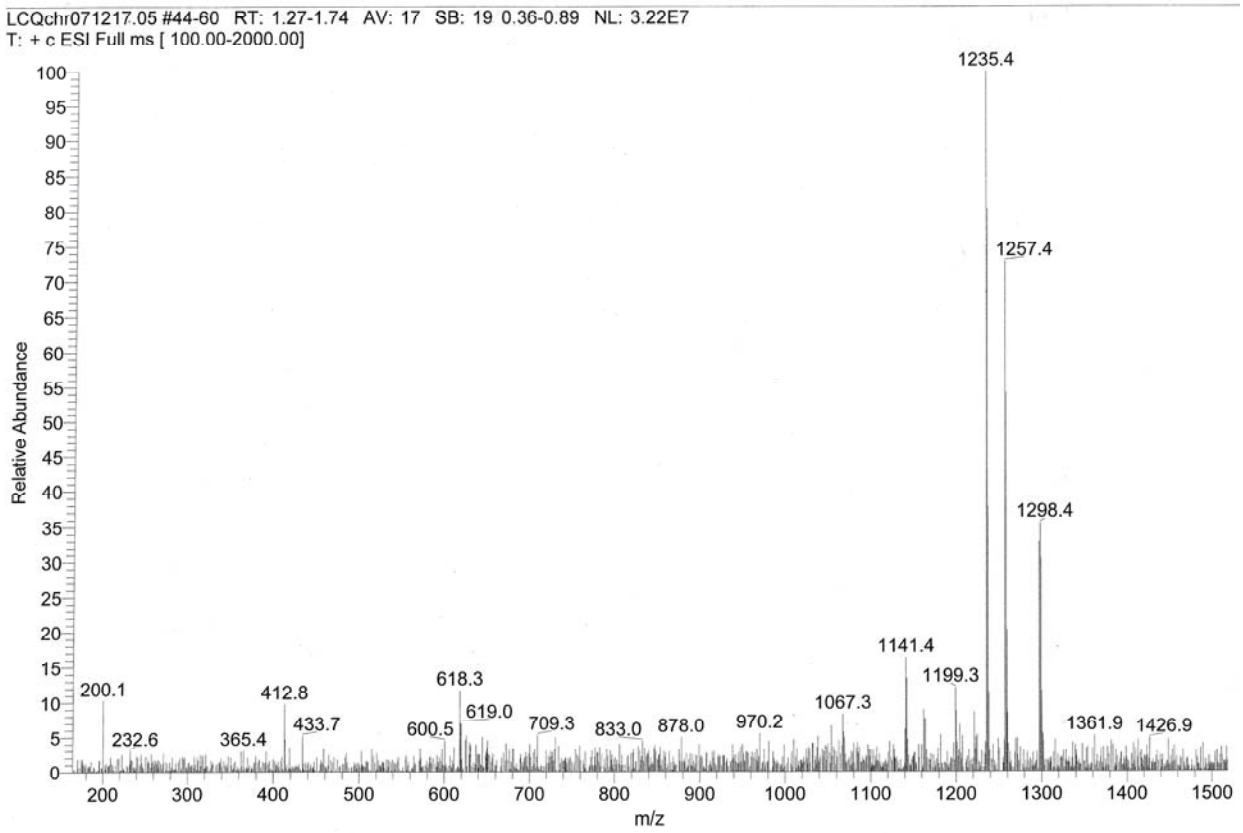

Figure S14: IR Spectrum of compound **3**

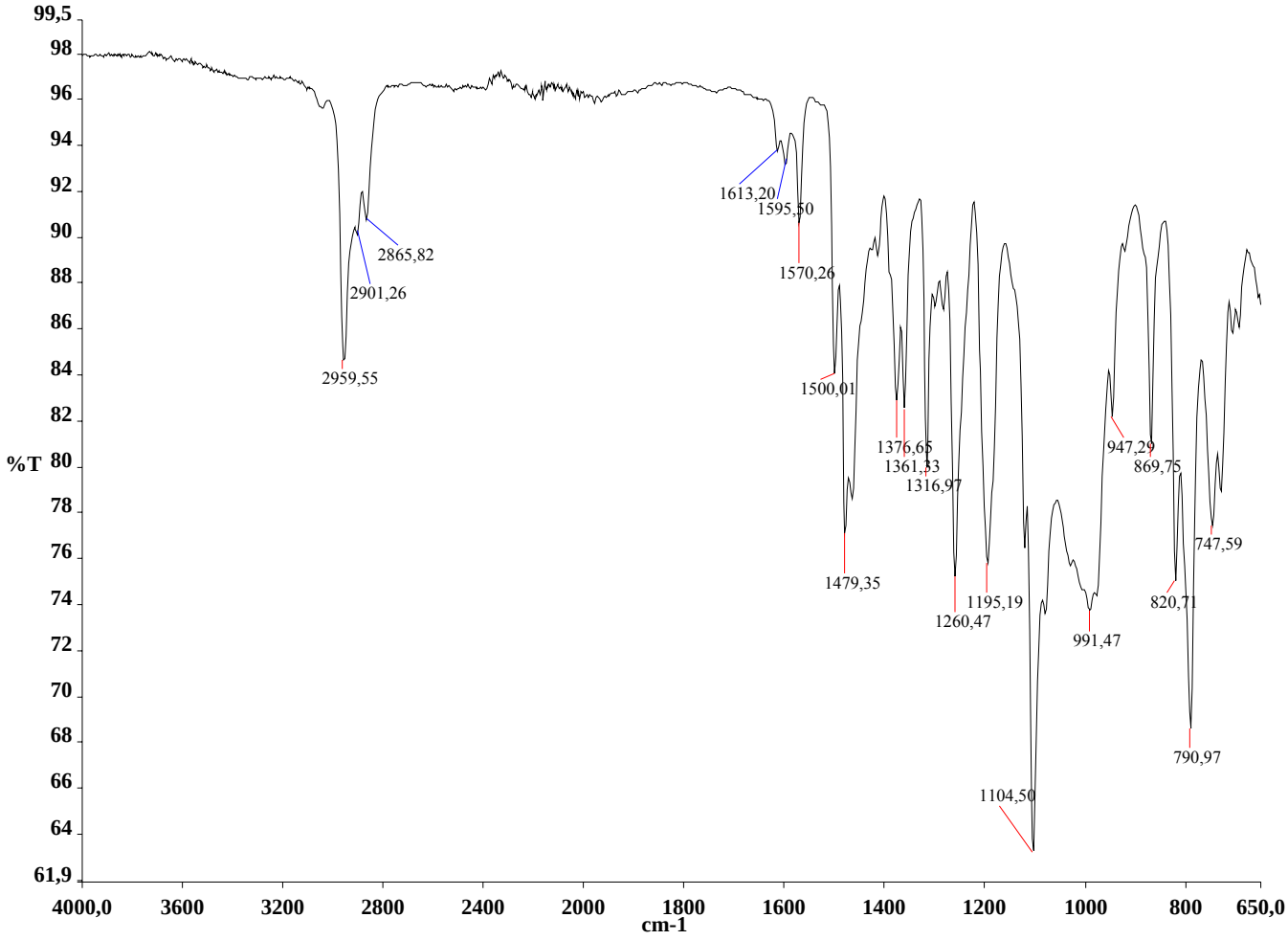

Figure S15: ^{1}H NMR Spectrum of compound **3.CuI**

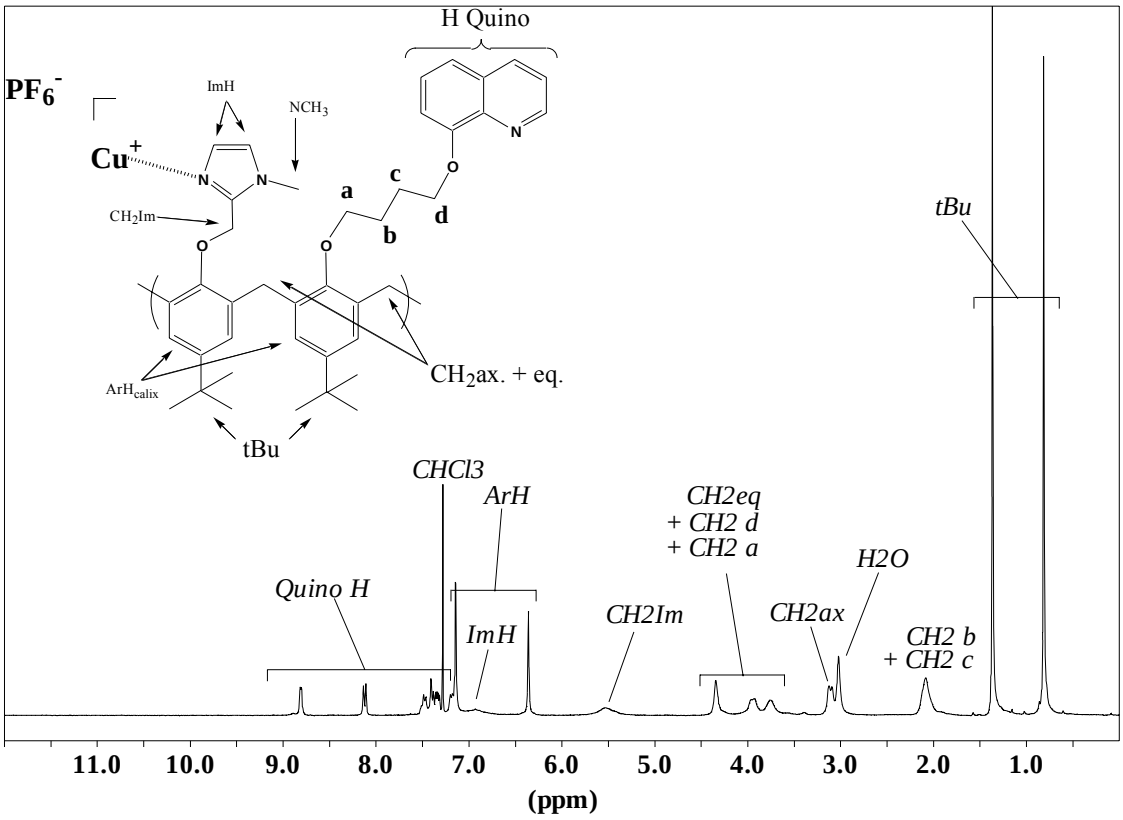

Figure S16: ^{13}C NMR Spectrum of compound **3.CuI**

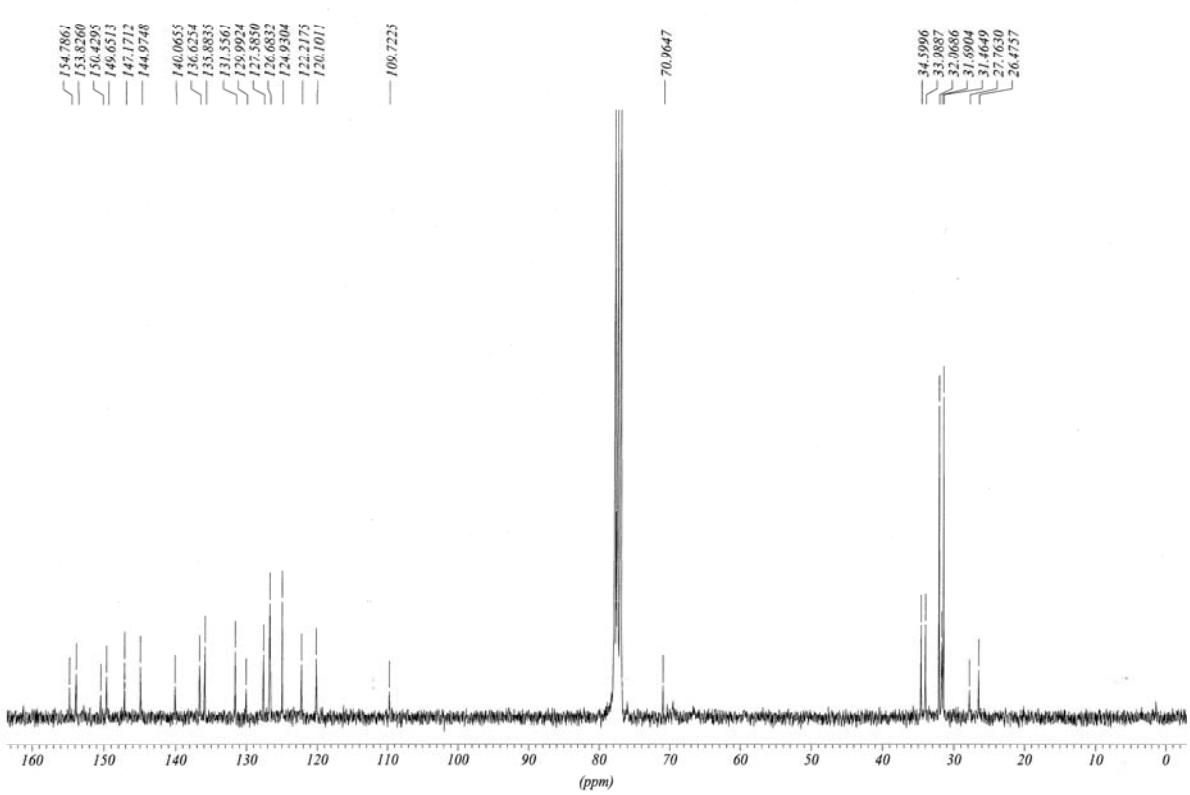

Figure S17: Mass Spectrum of compound **3.CuI**

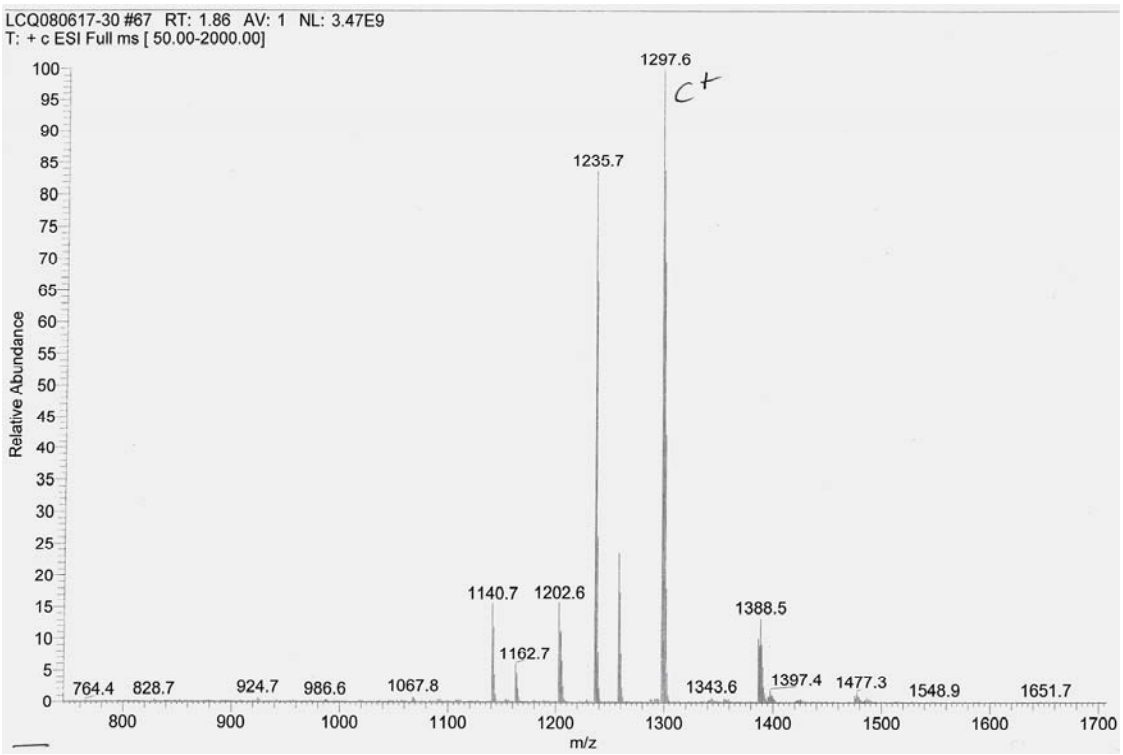

Figure S18: IR Spectrum of compound **3.CuI**

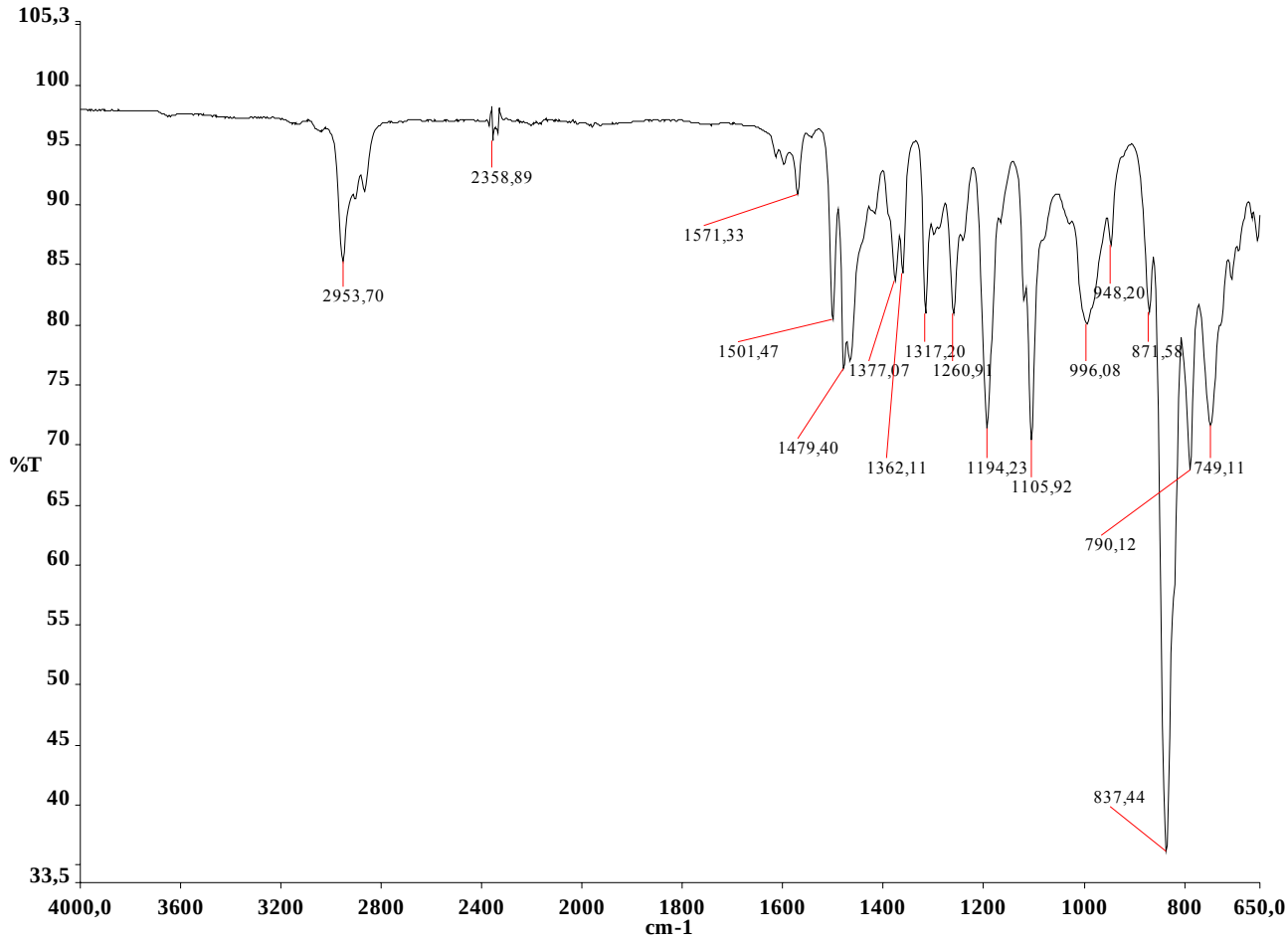

Figure S19: UV-vis Spectrum of compound **3.CuI** in an acetonitrile solution (10^{-3} M)

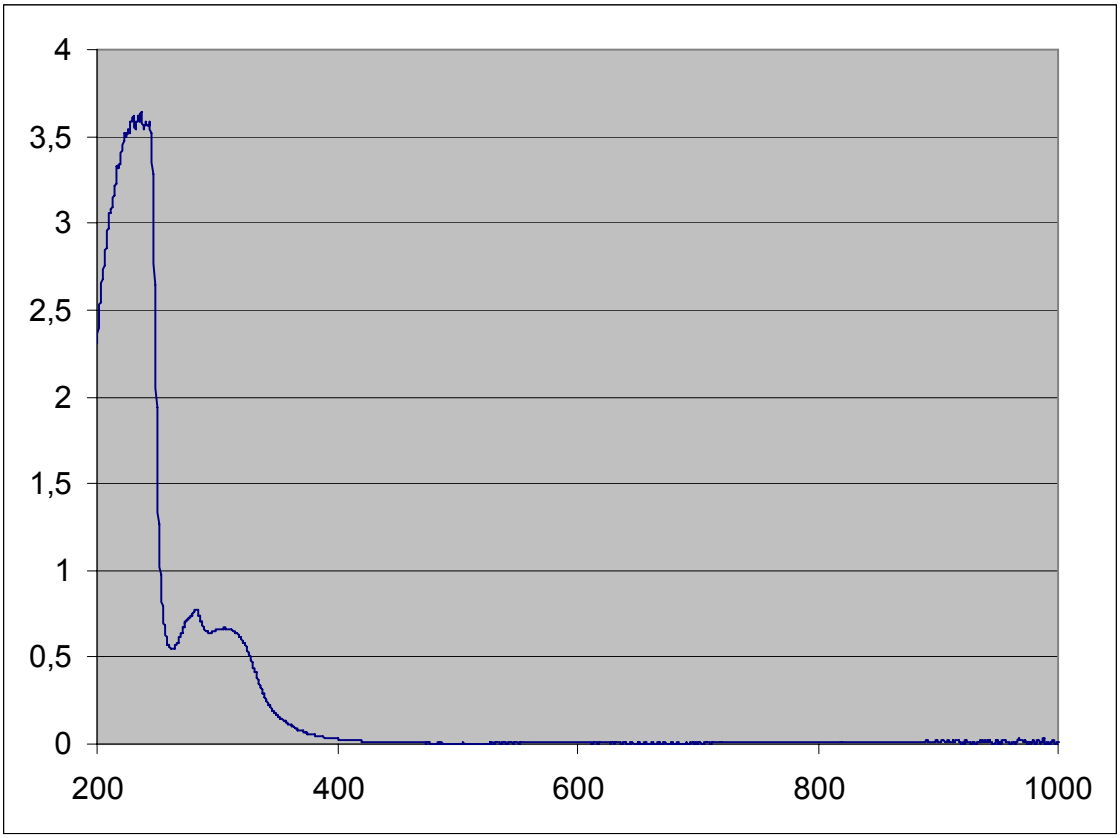

Figure S20: EPR Spectrum of compound **3.CuII**

EPR Spectrum, Freq. 9.44 GHz, Bruker EMX-plus spectrometer coupled with an Oxford Instrument Hélium cryostat. Frozen solution (1.45 mM) in CH_3CN/Toluène 1/1, v/v), T= 40K

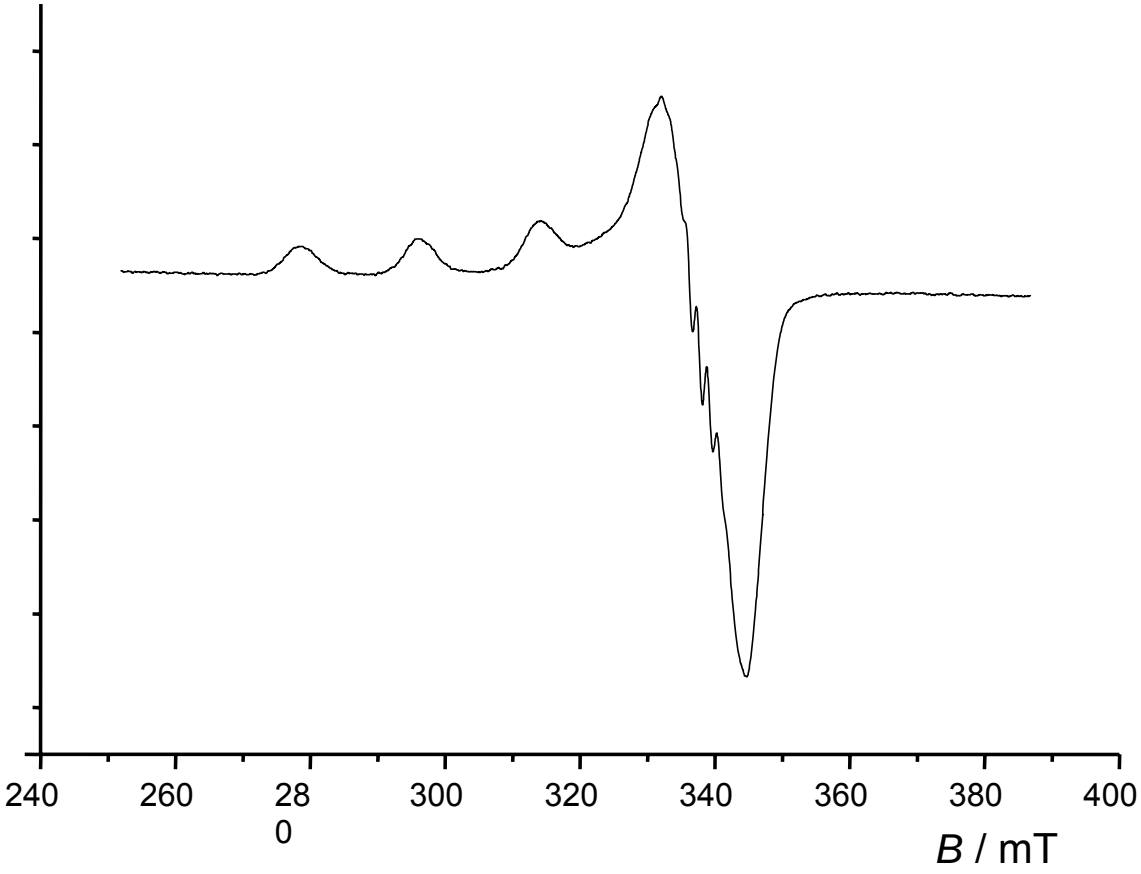

$A_{//} = 172\ 10^{-4}\ cm^{-1}$
$g_{//} = 2.211$
$g_{\perp} = 2.004$

Figure S21: Mass Spectrum of compound **3.CuII**

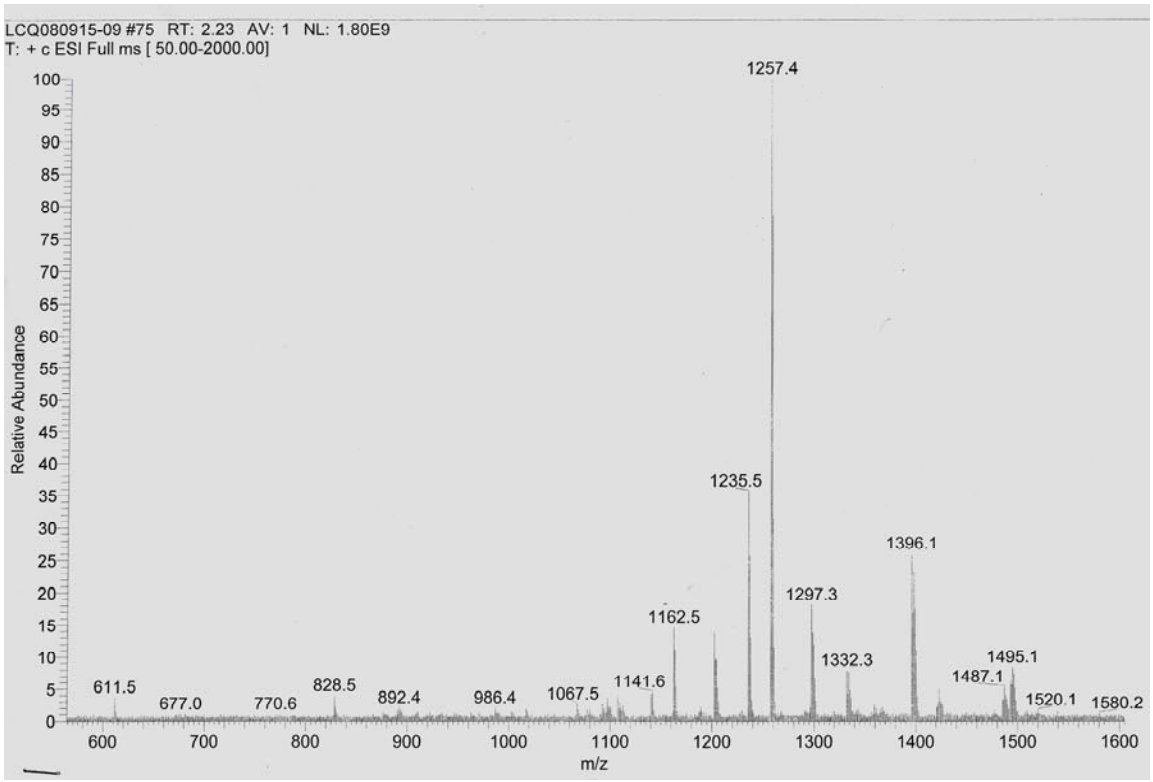

Figure S22: IR Spectrum of compound **3.CuII**

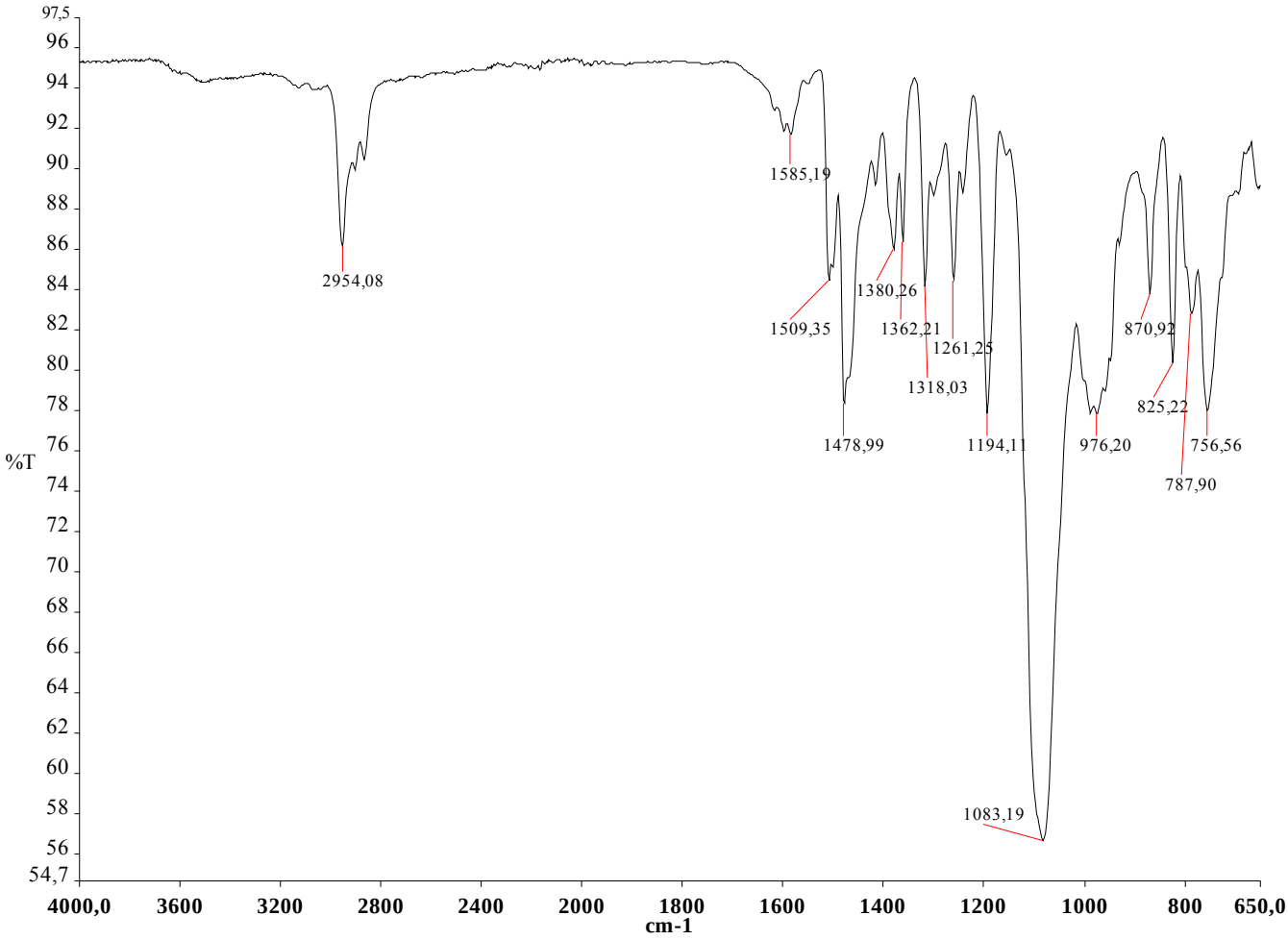

Figure S23: UV-vis Spectrum of compound **3.CuII.** Top: solid state, bottom: in acetonitrile solution (10-3 M)

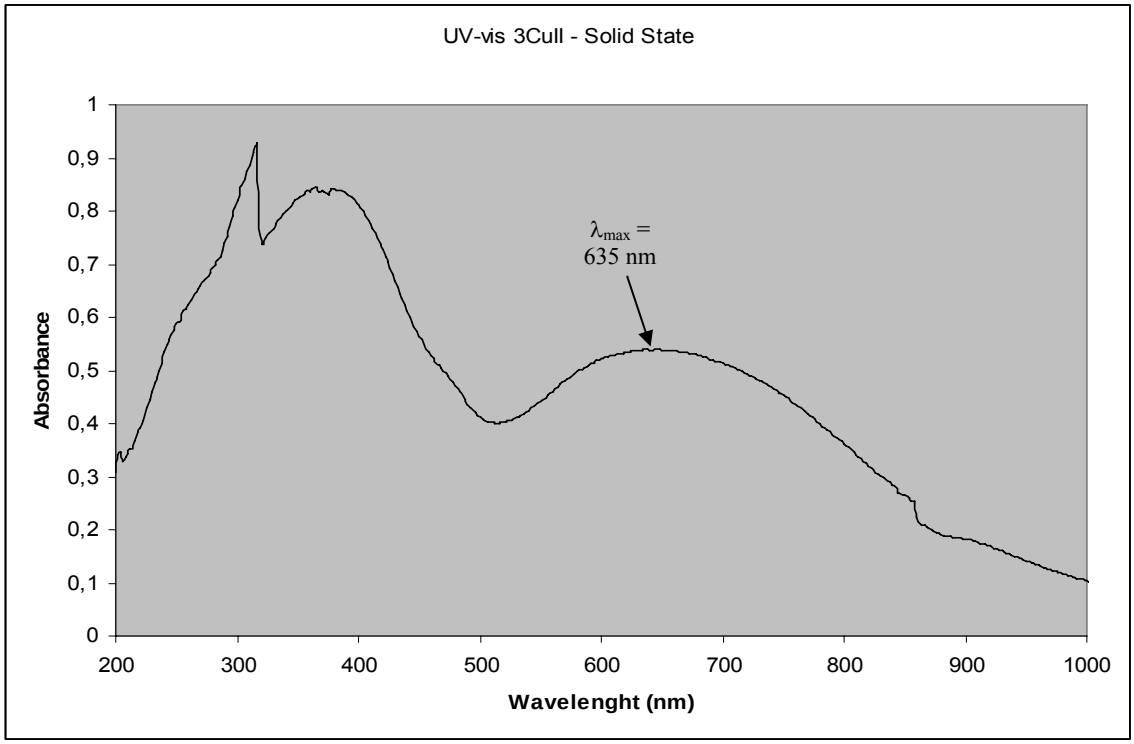

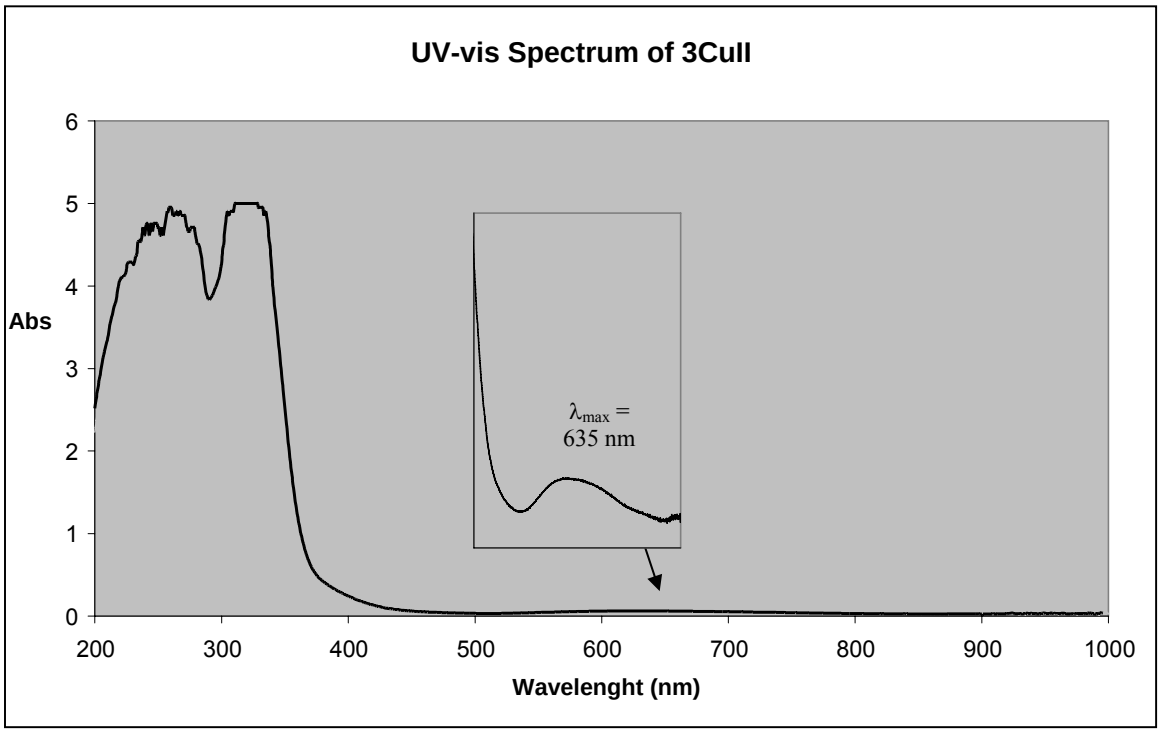

Figure S24: Dual display of ^{1}H NMR spectra of compounds **3** and **3.CuI**

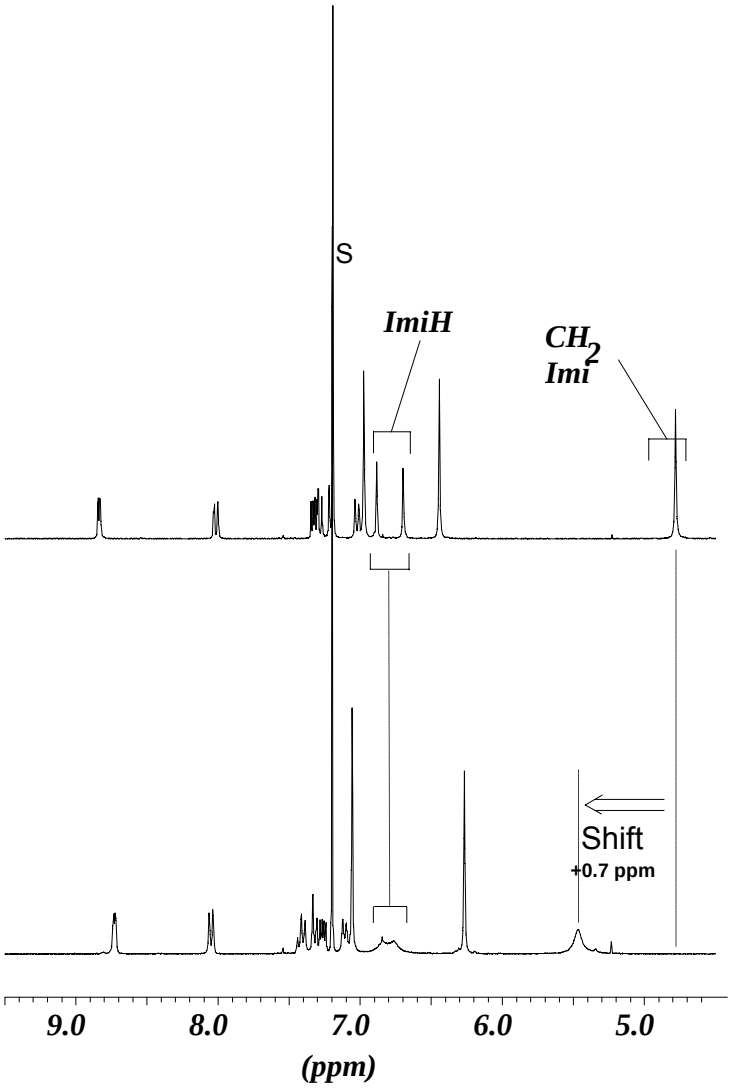

Figure S25: CV curves of [**3.**Cu(I)]$^{+}$ in CH_3CN + 0.1 M $TBAPF_6$ (0.1 $V.s^{-1}$, 1 mM, vitr. Carbon ø 2 mm, *E* vs Ag/Ag^{+}).

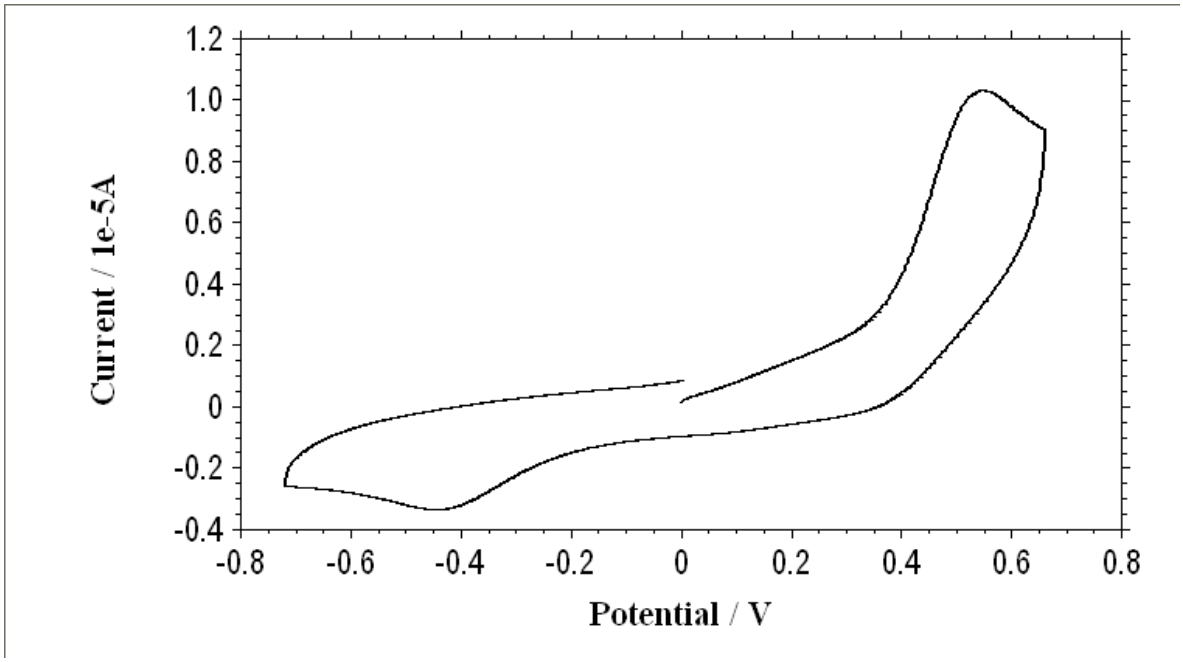

Figure S26: CV curves of [**3.**Cu(I)]$^{+}$ in CH_3CN + 0.1 M $TBAPF_6$ (1V.s^{-1}, 1 mM, vitr. carbon ø 2 mm, *E* vs Ag/Ag^{+}).

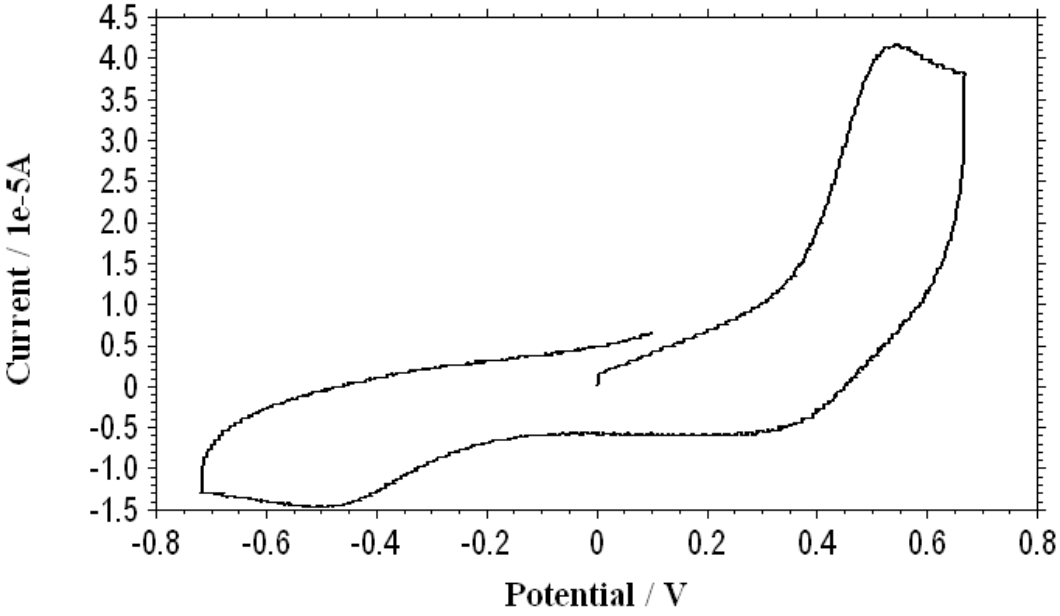

Figure S27: CV curves of [**3.**Cu(I)]$^{+}$ in CH_3CN + 0.1 M $TBAPF_6$ (5V.s^{-1}, 1 mM, vitr. carbon ø 2 mm, *E* vs Ag/Ag^{+}).

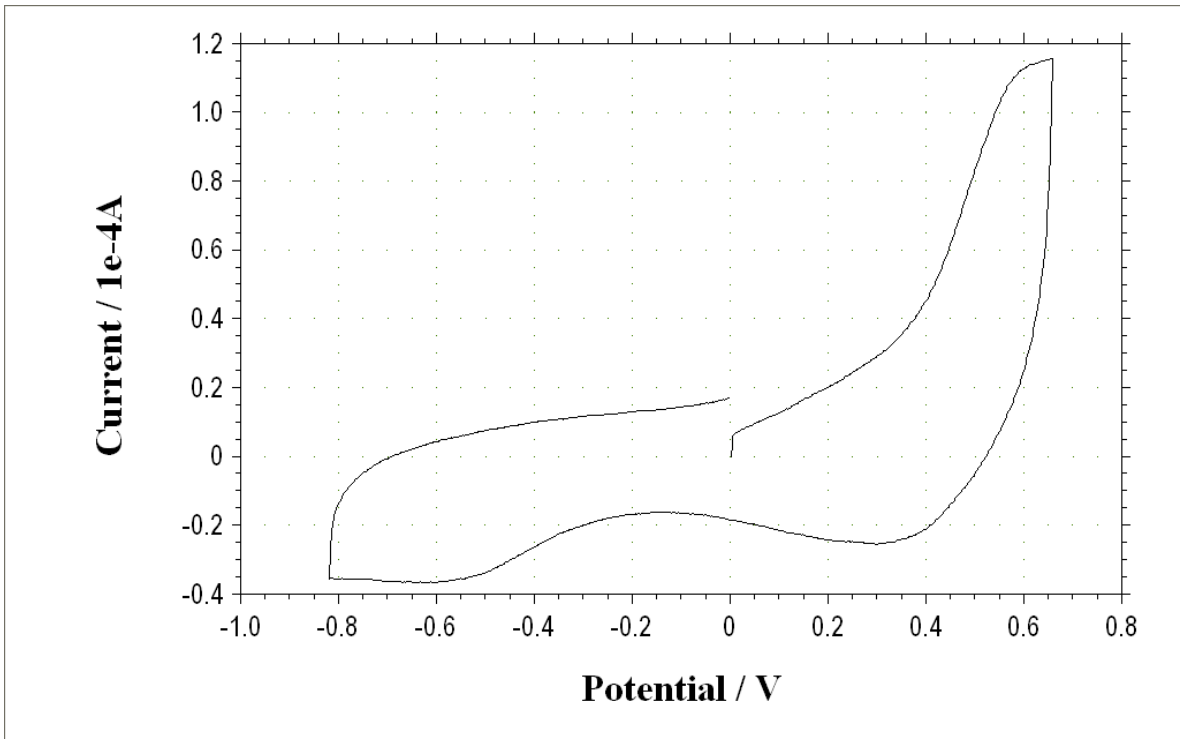

Figure S28: (*solid line*) Voltamperogram of [**3.**Cu(I)]$^{+}$ recorded with a vitreous carbon rotating disk in CH_3CN + 0.1 M $TBAPF_6$ (500 rd. s^{-1}, 10 $mV.s^{-1}$, 1 mM, vitr. carbon ø 2 mm, *E* vs Ag/Ag^{+}).
(c*rosses*) Voltamperogram recorded with a vitreous carbon rotating disk after bulk oxidation (carbon working electrode, E_{app} = 0.8 V) of [**3.**Cu(I)]$^{+}$ in CH_3CN + 0.1 M $TBAPF_6$ (500 rd. s^{-1}, 10 $mV.s^{-1}$, 1 mM, vitr. carbon ø 2 mm, *E* vs Ag/Ag^{+}).

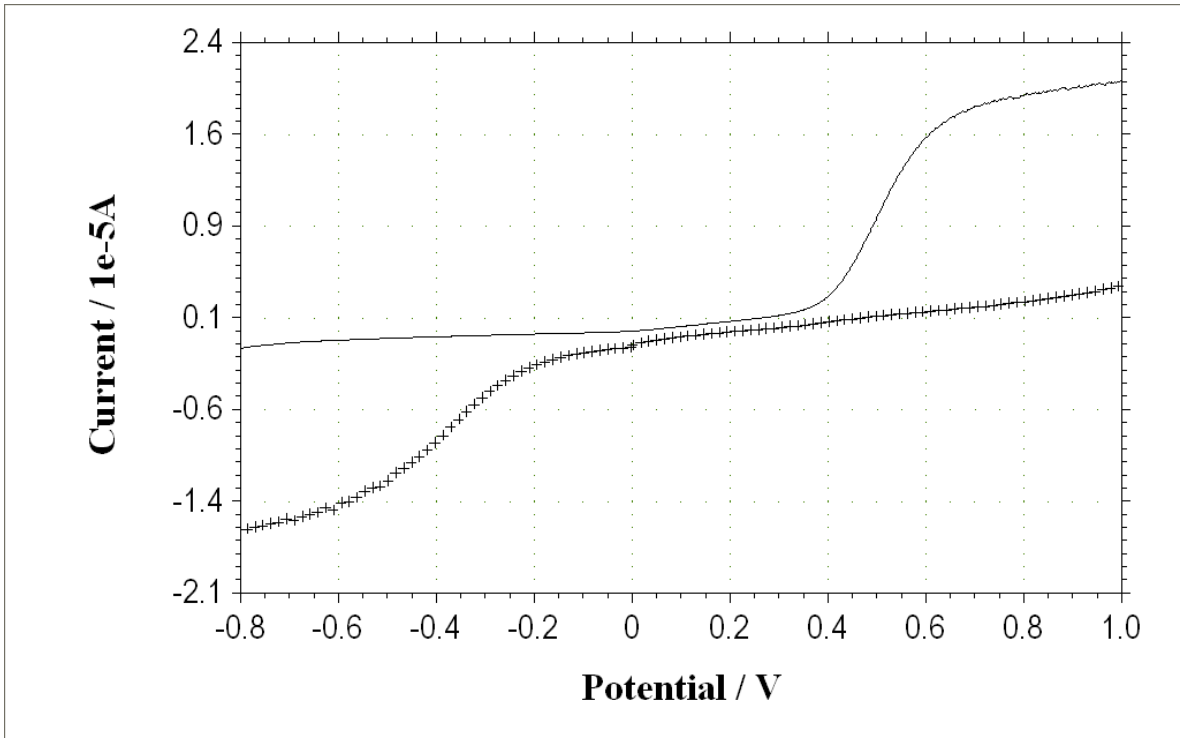

Figure S29: (*solid line*) CV curve of [**3.**Cu(I)]$^{+}$ recorded in CH_3CN + 0.1 M $TBAPF_6$ (100 $mV.s^{-1}$, 1 mM, vitr. carbon ø 2 mm, *E* vs Ag/Ag^{+}).
(c*rosses*) CV curve recorded after bulk oxidation (carbon working electrode, E_{app} = 0.8 V) of [**3.**Cu(I)]$^{+}$ in CH_3CN + 0.1 M $TBAPF_6$ (100 $mV.s^{-1}$, 1 mM, vitr. carbon ø 2 mm, *E* vs Ag/Ag^{+}).

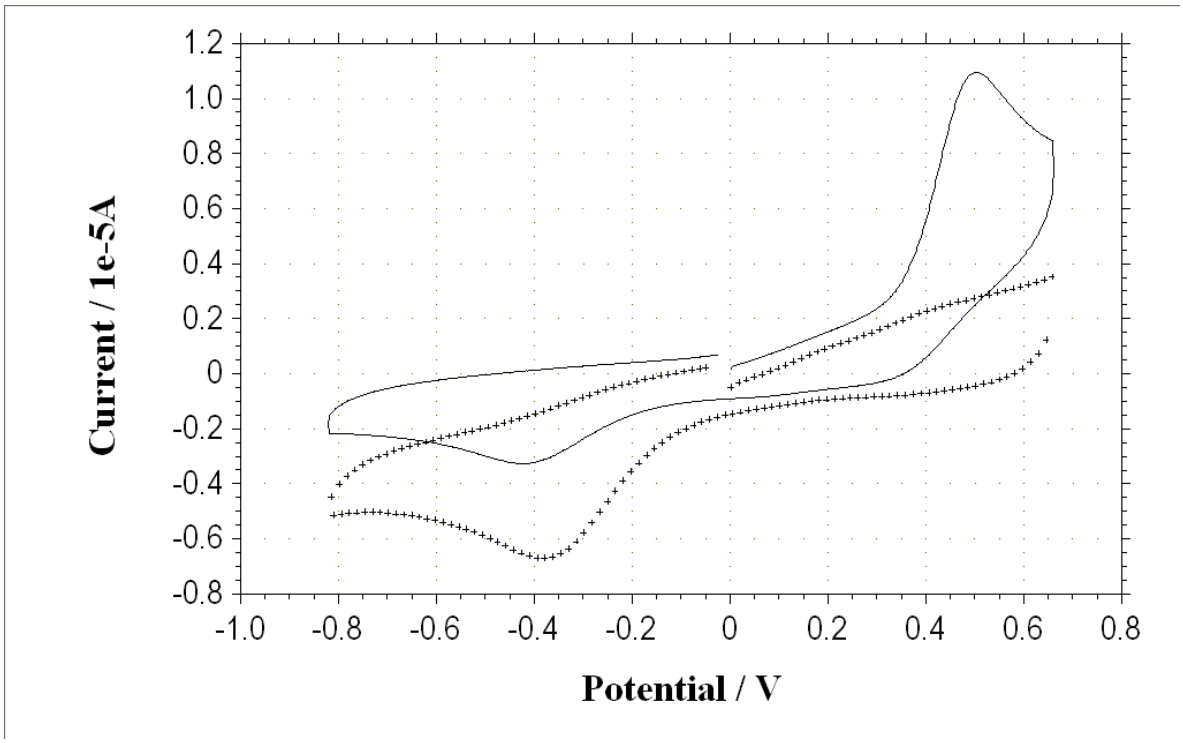

Figure S30: CV curve recorded after bulk oxidation (carbon working electrode, E_{app} = 0.8 V) of [**3.**Cu(I)]$^{+}$ in CH_3CN + 0.1 M $TBAPF_6$ (100 mV.s^{-1}, 1 mM, vitr. carbon ø 2 mm, *E* vs Ag/Ag^{+})

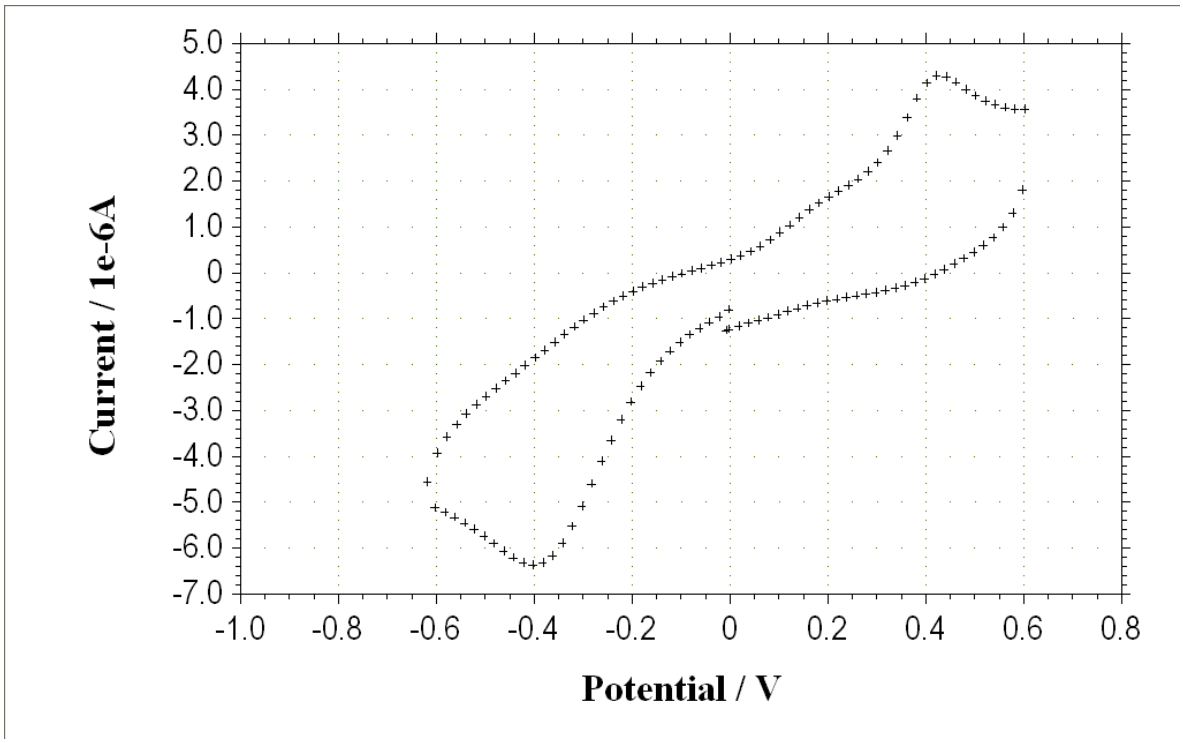

Figure S31: CV curves of [**3.**Cu(II)]$^{2+}$ in CH_3CN + 0.1 M $TBAPF_6$ (0.1 $V.s^{-1}$, 1 mM, vitr. carbon ø 2 mm, *E* vs Ag/Ag^{+}).

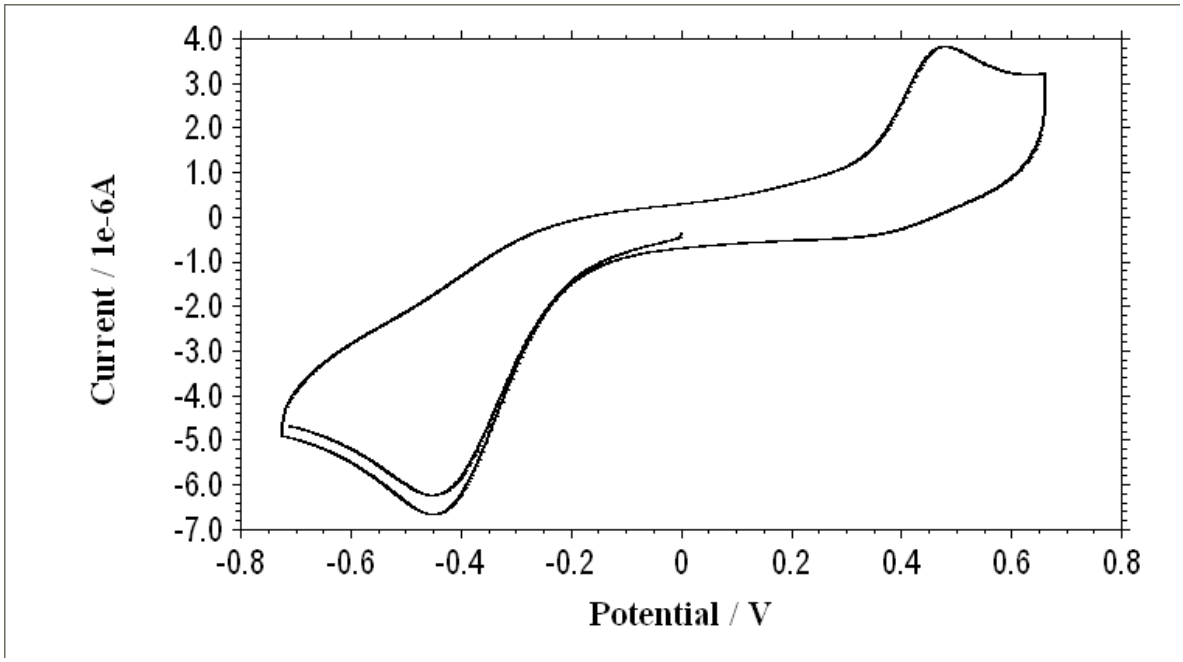

Figure S32: CV curves of [**3.**Cu(II)]$^{2+}$ in CH_3CN + 0.1 M $TBAPF_6$ (1 $V.s^{-1}$, 1 mM, vitr. carbon ø 2 mm, *E* vs Ag/Ag^+).

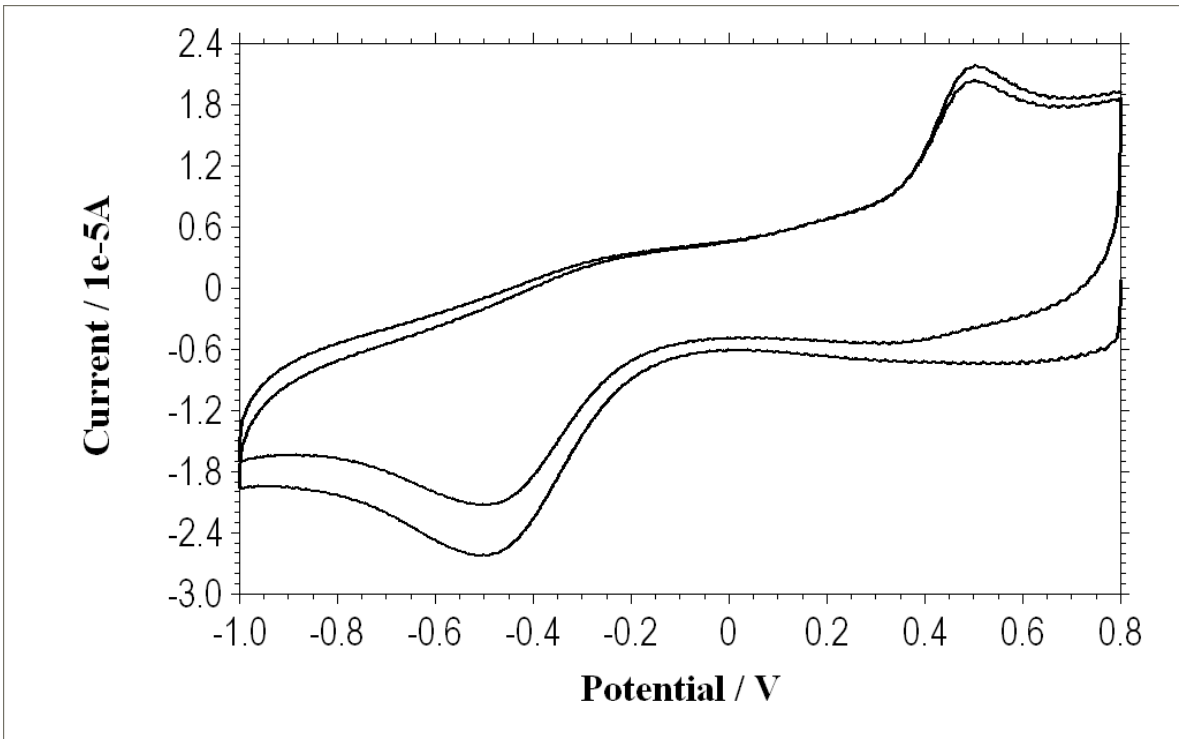

Figure S33: CV curves of [**3.**Cu(II)]$^{2+}$ in CH_3CN + 0.1 M $TBAPF_6$ (10 $V.s^{-1}$, 1 mM, vitr. Carbon ø 2 mm, *E* vs Ag/Ag^+).

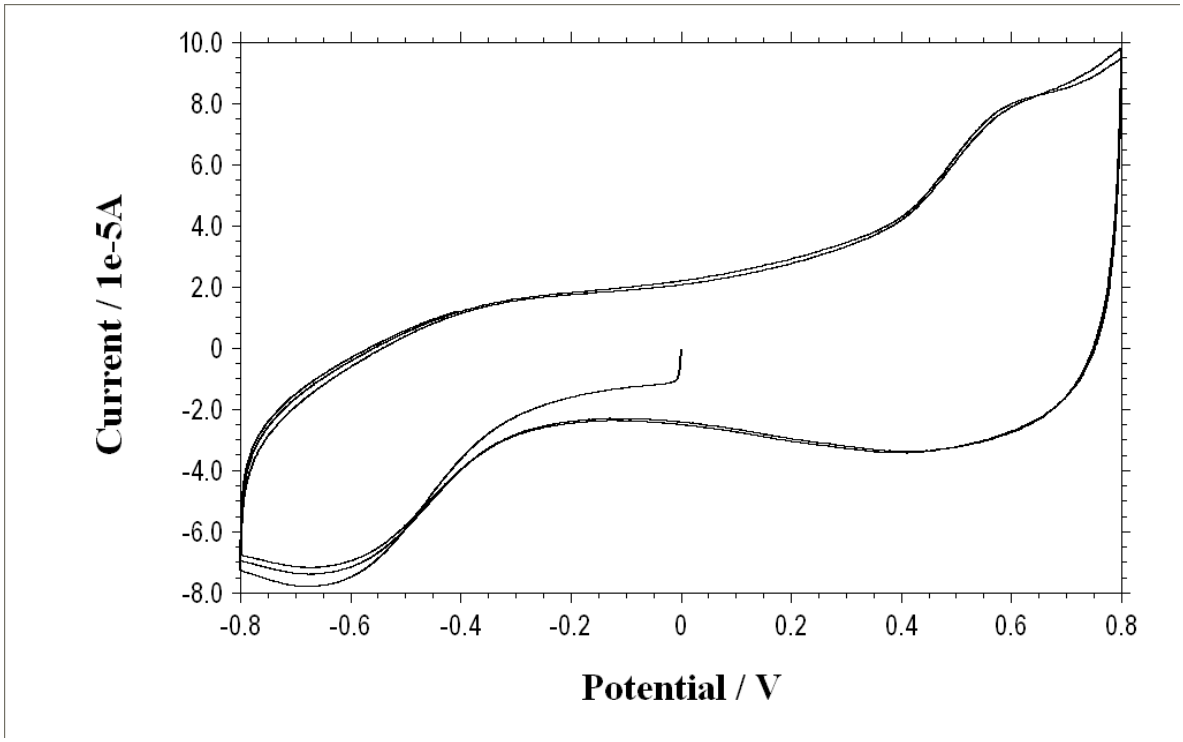

Figure S34: Voltamperogram recorded with a vitreous carbon rotating disk on [**3.**Cu(II)]$^{2+}$ in CH_3CN + 0.1 M $TBAPF_6$ (500 rd. s^{-1}, 10 $mV.s^{-1}$, 1 mM, vitr. carbon ø 2 mm, *E* vs Ag/Ag^+).

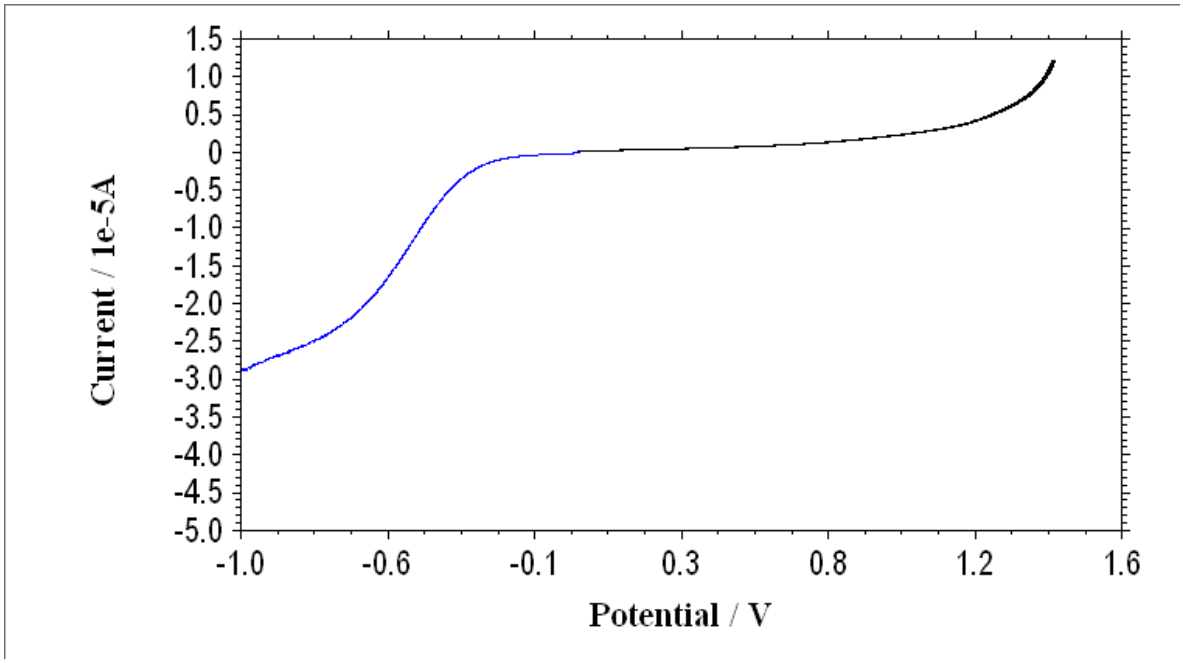

Figure S35: Reduction/oxidation cycles followed by UV-Vis spectroscopy (absorbance recorded at λ = 635 nm). Successive electrolyses (Q = 0.16 C) were carried out in a 1cm quartz cell starting from LCuI ($1x10^{-3}$ M in DMF, 0.1 M TBAP) upon switching the working electrode potential (1 cm^2 vitreous carbon) between + 0.6 and -0.6 V vs Ag/Ag^+.